

Nuclear and Particle Physics Research at the University of Richmond

Gerard P. Gilfoyle
Physics Department
University of Richmond
Richmond, VA, 23173 USA

November 23, 2004

Abstract

The central goal of the physics program at the Thomas Jefferson National Accelerator Facility (JLab) is to understand the transition from the hadronic picture of matter to one based on quarks and gluons. This focus here is the electrodisintegration of the deuteron at low energy (1 GeV) to establish a baseline for the hadronic picture so we can separate the effects of ‘conventional nuclear physics’ from quark-gluon ones at higher energy. Special features of the JLab electron beam and the detectors in Hall B will probe components of the deuteron wave function for the first time at these energies.

Contents

Task Introduction	5
Status Report	7
Task Description	15
References	24
Contract-Related Publications	27
Collaborating Institutions	29
Biographical Sketch	31
Special Considerations	34
Estimate of Unobligated Funds	34
Facilities and Resources	34
Current and Pending Support	34
Budget Explanation	35
Appendices	39
A - Compute node quote	39
B - Richmond Computing Cluster and Users	39
C - CLAS Approved Analysis proposal	43

1 Task Introduction

This is a renewal application for funding to support the University of Richmond (UR) electromagnetic nuclear physics research program in Hall B at the Thomas Jefferson National Accelerator Facility (JLab). Dr. Gerard P. Gilfoyle is the principle investigator (a previous co-principle investigator, Dr. Michael F. Vineyard is now at Union College in New York). Several other JLab collaborators use the Richmond computing cluster that is described below. In this Introduction I describe JLab and the Hall B detector, my physics goals, the objectives for the period of the proposed work and their expected significance, and summarize the accomplishments from the last grant period.

The Continuous Electron Beam Accelerator Facility (CEBAF) at Jefferson Lab provides a unique tool for basic research in nuclear physics. The central instrument of CEBAF is a superconducting electron accelerator with a maximum energy of 4-6 GeV, a 100% duty cycle, and a maximum current of 200 μA . These excellent beam characteristics allow for novel experiments that are being used to develop a quark-based, fundamental understanding of nuclei. The electron beam at CEBAF is used simultaneously for scattering experiments in three halls that contain complimentary experimental equipment. The primary instrument in Hall B is the CEBAF Large Acceptance Spectrometer (CLAS) [1] shown in Figure 1. This device is a toroidal, multi-gap magnetic spectrometer. The magnetic field is generated by six, iron-free superconducting coils. The particle detection system consists of drift chambers to determine the trajectories of charged particles, Cerenkov detectors for the identification of electrons, scintillation counters for time-of-flight measurements, and electromagnetic calorimeters to identify electrons and to detect photons and neutrons. The six segments are instrumented individually to form six independent spectrometers.

The CLAS detector was constructed and is operated by an international collaboration consisting of about thirty-five institutions. The CLAS Collaboration began production running in 1997 and a steady stream of physics publications has been established [2]. I have been part of the CLAS Collaboration since its inception, and I have been actively involved in the construction of the spectrometer and the development of the physics program.

The focus of my physics goals is to study the nucleon-nucleon force in the transition region where the hadronic picture of nuclei gives way to quark-gluon degrees of freedom. This is one of the ‘central problems of modern science’ described in the long-range plan of the Nuclear Science Advisory Committee (NSAC) [3]. In particular, I am investigating the electrodisintegration of the deuteron (the $d(\vec{e}, e'p)n$ reaction) in the 1 GeV region using the out-of-plane production of the ejected proton and taking advantage of the unique, almost- 4π acceptance of CLAS. These out-of-plane measurements are significant because they provide a unique opportunity to probe components of the deuteron wave function that are difficult or impossible otherwise. In particular, the fifth structure function f'_{LT} , the imaginary part of the longitudinal-transverse interference of the electromagnetic current, is non-zero only for out-of-plane production. The out-of-plane production can be used to also study other parts of the deuteron structure functions namely the longitudinal-transverse (f_{LT}) and transverse-transverse (f_{TT}) parts of the electromagnetic current. I will be focusing on the quasi-elastic peak and at higher energy transfer in the dip region. No other measurements like these exist in this energy region. See Section 2.1 for a status report and Section 3.1 for a detailed plan of work. This project will establish a baseline for the hadronic picture of matter so we

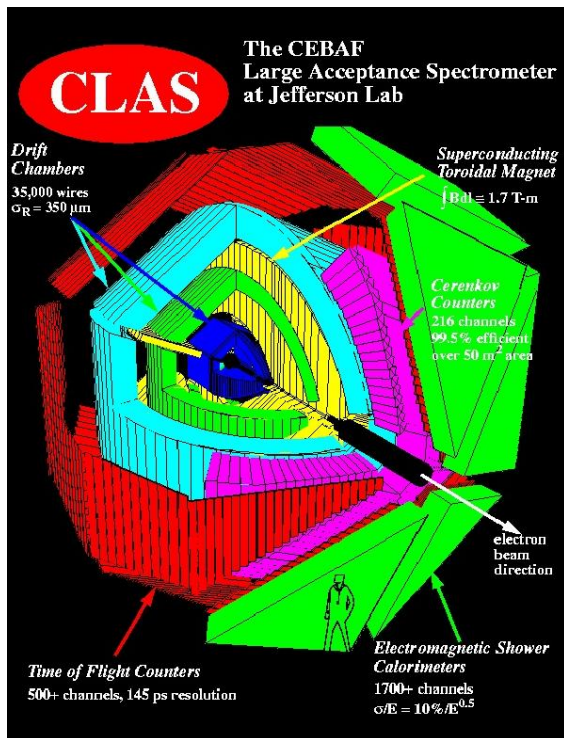


Figure 1: The CEBAF Large Acceptance Spectrometer (CLAS).

can clearly separate the effects of ‘conventional nuclear physics’ from quark-gluon degrees of freedom at higher energy [4, 5, 6, 7]. The geography of this transition region is complex and discriminating between the two pictures remains a challenge [8, 9].

I now summarize the the work of the last grant period. The analysis of the $d(\vec{e}, e'p)n$ reaction was started since my last grant renewal in 2001 and it will use existing data (from the E5 running period and others). The project was approved by the CLAS Collaboration in November, 2003. The CLAS Collaboration has a procedure for reviewing and judging analysis projects that is similar to the process used for evaluating beam time proposals. An analysis proposal is presented and approved by one of the physics working groups and then goes before the entire Collaboration for discussion and approval. A status report is in Section 2.1. See Appendix C for the CLAS Approved Analysis proposal.

Another experiment entitled (*Measurements of the Electroproduction of the Λ , $\Lambda^*(1520)$, and $f_0(975)$ via the $K^+\pi^-p$ and K^+K^-p Final States*) was completed with a negative result (see last annual report). No evidence of the $f_0(980)$ scalar meson was observed. It is worth noting the final phase of this project was done almost entirely by one of my undergraduates.

In the last three years I have developed a computing cluster at the University of Richmond consisting of 53, dual-CPU computers supported by 4.5 TByte of storage. Funds for the system were obtained from the National Science Foundation’s Major Research Instrumentation (MRI) program and the University. The computing cluster is used by me and other collaborators at JLab. Funds are requested in this proposal to replace some of the aging computing nodes to enhance the cluster performance and improve research productivity. More details are in Section 2.2.2 and Section 3.3.

My CLAS Collaboration service work in the last three years includes developing a code that performs more complete calculations of radiative corrections for electron scattering off the deuteron. These calculations are fully exclusive ones and do not suffer from the limitations of past calculations. This project is discussed in more detail in Sections 2.2.1 and 3.2. I am also responsible for online monitoring of CLAS data quality (see Sections 2.2.3 and 3.2).

As always, undergraduate students will be involved in all phases of this research program (Richmond is a primarily undergraduate institution). The involvement of these students in research as part of their undergraduate education is an important part of the process of recruiting and training bright young people for careers in science. The Department of Physics at UR is dedicated to this process. Five different students have participated in nuclear physics research with me funded by DOE in the last three years. See Section 3.5 for more details.

2 Status Report of Current Projects

2.1 Out-of-Plane Measurements of Deuteron Structure Functions

I discuss here a new analysis project to study existing CLAS data and extract the structure functions f_{LT} , f_{TT} , and f'_{LT} of the deuteron using the proton azimuthal distribution from the $d(\vec{e}, e'p)n$ reaction. The formalism used to describe the electromagnetic response of the deuteron is presented first followed by a discussion of the current state of the analysis.

2.1.1 Formalism

For the case of a polarized electron beam incident on an unpolarized target, the three-fold differential cross section can be written in the one-photon exchange approximation as

$$\frac{d^3\sigma}{d\nu d\Omega_e d\Omega_p} = c\{\rho_L f_L + \rho_T f_T + \rho_{LT} f_{LT} \cos(\phi_{pq}) + \rho_{TT} f_{TT} \cos(2\phi_{pq}) + h\rho'_{LT} f'_{LT} \sin(\phi_{pq})\} \quad (1)$$

where

$$c = \frac{\alpha E'}{6\pi^2 Q^4 E}, \quad (2)$$

α is the fine-structure constant, E and E' are the incoming and outgoing electron energies respectively, Q^2 is the square of the 4-momentum transfer, h is the electron beam helicity (± 1), the $\rho_{\lambda\lambda'}$ are the virtual-photon density matrix elements which depend only on the electron kinematics, and the $f_{\lambda\lambda'}$ are the response functions in the center of mass [10]. The azimuthal angle ϕ_{pq} is the angle between the scattering plane defined by the incoming and outgoing electrons and the reaction plane defined by the ejected proton and neutron (see Figure 2). The response functions depend on the energy transfer ν , the 3-momentum transfer \vec{q} , and θ_{pq}^{cm} where θ_{pq}^{cm} is the angle between \vec{q} and the ejected proton momentum in the center-of-mass frame (see Figure 2). The missing momentum is often used to describe this reaction and is defined as

$$\vec{p}_m = \vec{q} - \vec{p}_p \quad (3)$$

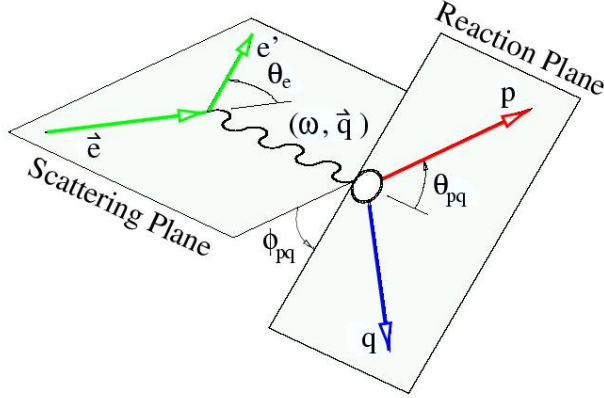


Figure 2: Kinematic quantities for $d(\vec{e}, e'p)n$.

where \vec{p}_p is the ejected proton momentum. In the plane-wave impulse approximation this missing momentum is the opposite of the initial momentum of the proton.

The conventional approach to extracting the response functions in Equation 1 is to use the asymmetries defined below [11, 12, 13, 14].

$$A_{LT} = \frac{\sigma_{0^\circ} - \sigma_{180^\circ}}{\sigma_{0^\circ} + \sigma_{180^\circ}} = \frac{\rho_{LT} f_{LT}}{\rho_L f_L + \rho_T f_T + \rho_{TT} f_{TT}} \quad (4)$$

$$A'_{LT} = \frac{\sigma_{90^\circ}^{(+)} - \sigma_{90^\circ}^{(-)}}{\sigma_{90^\circ}^{(+)} + \sigma_{90^\circ}^{(-)}} = \frac{\rho' f'_{LT}}{\rho_L f_L + \rho_T f_T - \rho_{TT} f_{TT}} \quad (5)$$

$$A_{TT} = \frac{\sigma_{0^\circ} + \sigma_{180^\circ} - 2\sigma_{90^\circ}}{\sigma_{0^\circ} + \sigma_{180^\circ} + 2\sigma_{90^\circ}} = \frac{\rho_{TT} f_{TT}}{\rho_L f_L + \rho_T f_T} \quad (6)$$

The subscripts refer to the value of ϕ_{pq} and the superscripts refer to the beam helicity. These equations can be rearranged to calculate the response functions (see Appendix C Section 2). The advantage of using asymmetries is that dividing by a sum of response functions reduces the sensitivity to systematic errors. This is particularly true for Equation 5 for A'_{LT} where the cross sections are all measured at the same place and the differ only by the properties of the beam (the helicity). The other two asymmetries A_{LT} and A_{TT} do not share this feature. In Section 2.1.2 I discuss how to use the large acceptance of CLAS to measure the asymmetries in Equations 4-6.

2.1.2 Preliminary Analysis Results

The analysis of the quasi-elastic deuteron structure functions using the out-of-plane production in the $d(\vec{e}, e'p)n$ reaction has begun. The scattered electron and the ejected proton are measured with CLAS and the missing mass technique is used to identify the neutron. The data were collected during the E5 run period and consist of runs 24020-24588. About 2.3 billion triggers were collected under three sets of run conditions: (1) $E_{beam} = 4.23$ GeV,

$I_{torus} = 3375$ A, normal polarity (inbending electrons), (2) $E_{beam} = 2.56$ GeV, $I_{torus} = 2250$ A, normal polarity, and (3) $E_{beam} = 2.56$ GeV, $I_{torus} = 2250$ A, reversed polarity (outbending electrons) to reach lower Q^2 . The Q^2 range is about $0.2 - 4.0$ (GeV/c)². See Figure 3 for a plot of the acceptance for the three sets of running conditions. A dual-target was

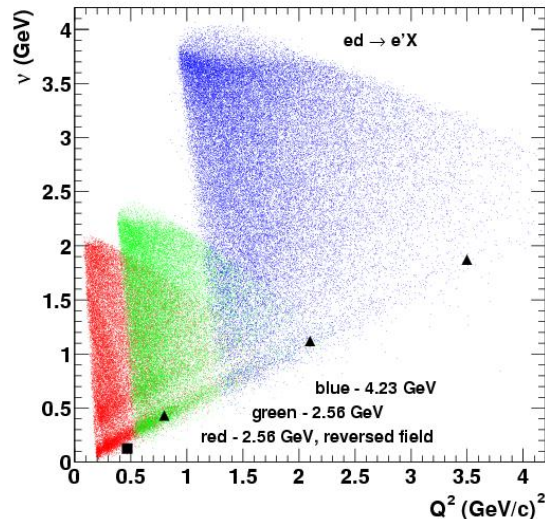


Figure 3: Energy loss of the electron versus Q^2 . The red, green, and blues areas represent the kinematic coverage for the three running conditions during the E5 run period. The triangles are the kinematics for the measurement of σ_{LT} for E01-020. The square is the anticipated kinematics for E02-101.

used consisting of collinear hydrogen and deuterium targets so calibrations could be done *in situ* and consistency checks could be preformed using the hydrogen target simultaneously with data collection on deuterium.

Data selection, kinematic cuts, and corrections have followed previous analyses of CLAS data. Significant progress has been made. Electrons and protons can be identified cleanly and missing mass is used to reconstruct the neutrons. Improvements in fiducial cuts and the determination of the electron momentum are in progress. More details on the methods are described in references [15, 16, 17, 18, 19] and in the CLAS Approved Analysis proposal in Appendix C [20].

One of the conventional methods for determining the response functions uses the asymmetries defined in Equations 4-6. Those asymmetries use small angle bins. In this work I want to take full advantage of the large acceptance of CLAS. Consider A'_{LT} first. The same asymmetry can be extracted using the weighted average

$$\langle \sin \phi_{pq} \rangle_{\pm} = \frac{\int_0^{2\pi} \sigma^{\pm} \sin \phi_{pq} d\phi_{pq}}{\int_0^{2\pi} \sigma^{\pm} d\phi_{pq}} \quad (7)$$

where the \pm refers to the beam helicity. In Appendix C, Section 4.3 I show that

$$\langle \sin \phi_{pq} \rangle_{+} - \langle \sin \phi_{pq} \rangle_{-} = \frac{\rho'_{LT} f'_{LT}}{\rho_L f_L + \rho_T f_T} \approx A'_{LT} \quad (8)$$

where the approximation that f_{TT} is small compared to f_L and f_T has been used. Thus, the asymmetry A'_{LT} associated with f'_{LT} can be extracted using the full acceptance of CLAS instead of small angle bins as in conventional spectrometers. Preliminary results for A'_{LT} using this method are shown in Figure 4. This result is averaged over the full Q^2 range

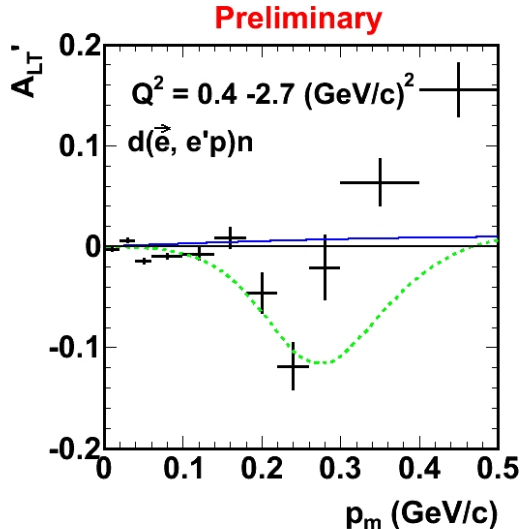


Figure 4: Fifth structure function asymmetry for $E = 2.56 \text{ GeV}$, normal torus polarity, and quasielastic kinematics.

$(0.4 - 2.7 \text{ (GeV/c)}^2$ for the 2.56-GeV, normal-torus-polarity running conditions and corrected for the CEBAF beam polarization. The data have not been corrected for acceptance or radiative effects. There are three distinct features in the asymmetry. For $p_m < 150 \text{ MeV/c}$, A'_{LT} is small. There is a significant ($\approx 5\sigma$) dip at $p_m \approx 240 \text{ MeV/c}$ followed by a steady rise for $p_m > 350 \text{ MeV/c}$. The curves in Figure 4 are from two calculations by S.Jeschonnek (solid, blue curve) and H.Arenhövel (dashed, green curve). The calculation by S.Jeschonnek is a relativistic one and includes final state interactions [21]. The one by H.Arenhövel is a low-energy calculation that includes final-state interactions, meson-exchange currents, relativistic corrections, and isobar configurations [22]. It is valid only up to about 1 GeV so the data shown in Figure 4 are at the limit and above the range of validity of the calculation. Neither calculation has been averaged over the CLAS acceptance. The significant differences between the data and the calculations demonstrate the need to improve our understanding of the electromagnetic structure of the deuteron. It is worth noting the quality of the data. The asymmetry A'_{LT} has been measured at statistically significant (5σ) levels out to large missing momentum.

For the LT and TT response functions analogous methods can be used. To get A_{LT} consider

$$\langle \cos \phi_{pq} \rangle = \frac{\int_0^{2\pi} \sigma^\pm \cos \phi_{pq} d\phi_{pq}}{\int_0^{2\pi} \sigma^\pm d\phi_{pq}} = \frac{\rho_{LT} f_{LT}}{2(\rho_L f_L + \rho_T f_T)} \approx \frac{A_{LT}}{2} \quad (9)$$

and for A_{TT} use

$$\langle \cos 2\phi_{pq} \rangle = \frac{\int_0^{2\pi} \sigma^\pm \cos 2\phi_{pq} d\phi_{pq}}{\int_0^{2\pi} \sigma^\pm d\phi_{pq}} = \frac{\rho_{TT} f_{TT}}{2(\rho_L f_L + \rho_T f_T)} \approx \frac{A_{TT}}{2} \quad (10)$$

where the same approximation as before has been used that the contribution of f_{TT} is small compared with f_L and f_T . Preliminary results are shown in Figure 5. In each case the

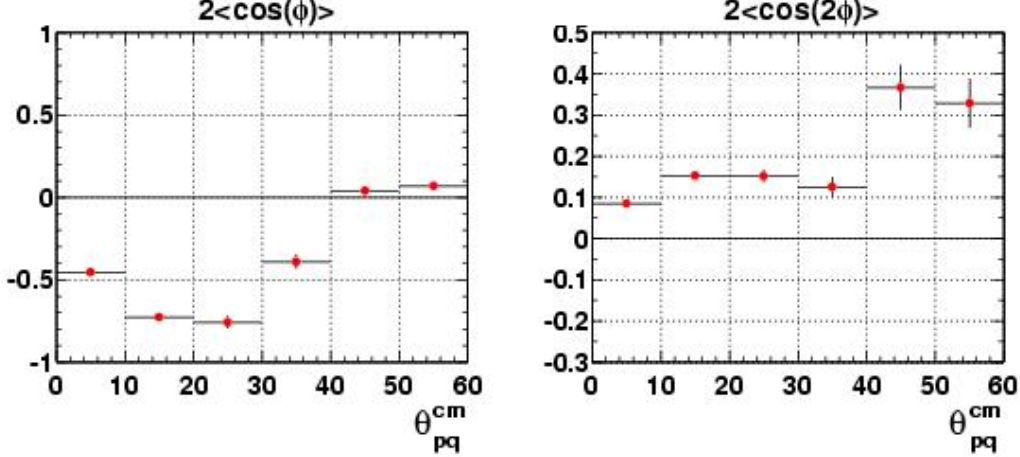


Figure 5: Structure function asymmetries for $E = 2.56 \text{ GeV}$, normal torus field, polarity, quasi-elastic kinematics. The left-hand panel displays A_{LT} , the right-hand one displays A_{TT} .

amplitudes are large and the statistical accuracy is quite good.

I have applied several tests of the analysis so far. Consider the helicity asymmetry

$$A(\phi_{pq}) = \frac{\sigma^+ - \sigma^-}{\sigma^+ + \sigma^-} \approx A'_{LT} \sin \phi_{pq} \quad (11)$$

where the superscripts refer to the beam helicity and the contribution of f_{LT} and f_{TT} relative to f_T and f_L have been neglected (see Appendix C, Section 4.3). The helicity asymmetry can then be fitted with a sine function to extract A'_{LT} . Our results show the two methods are perfectly consistent with one another (see Appendix C, Figure 13).

Another consistency check has been applied to the algorithm for extracting A'_{LT} using earlier CLAS results and is shown in Figure 6. Recall that with the E5 dual-target data is collected on deuterium and hydrogen simultaneously. In a previous CLAS experiment data were collected on the $p(\vec{e}, e'p)\pi^0$ reaction and a similar analysis of A'_{LT} was performed. In that work, K.Joo, *et al.* used the average A'_{LT} from $p(\vec{e}, e'p)\pi^0$ extracted run-by-run as a monitoring tool [23]. The same procedure was followed here using the scattering from the proton target and the same algorithms used in the deuterium analysis modified for $p(\vec{e}, e'p)\pi^0$ reaction. The results for the analysis of the E5 data set are shown in Figure 6. The E5 results are for a different range of Q^2 and different beam energy (and ϵ) than the analysis of K.Joo, *et al.* Nevertheless, the E5 results are in agreement in both sign and magnitude with the ones of K.Joo, *et al.* The E5 average A'_{LT} is -0.0154 ± 0.0017 versus -0.0158 ± 0.0009 for K.Joo, *et al.* This result implies our algorithms for extracting A'_{LT} are consistent with previous work.

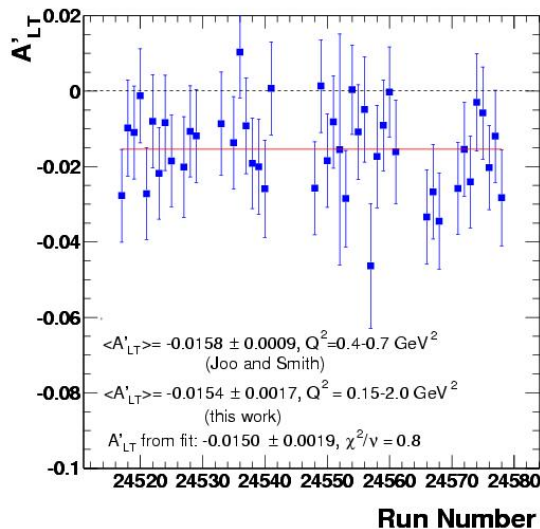


Figure 6: Run-by-run measurement of A'_{LT} from the $p(\vec{e}, e'p)\pi^0$ reaction for $E = 2.56 \text{ GeV}$ (normal torus field polarity). This result is consistent with the results of K.Joo, *et al.* [23].

2.2 CLAS Collaboration Service

2.2.1 Radiative Corrections for $d(\vec{e}, e'p)n$

The measurements of the $d(\vec{e}, e'p)n$ reaction in the E5 running period are subject to radiative corrections. In this section, a new code called EXCLURAD for calculating these corrections is described which can be used for exclusive reactions using electrons. The new program was modified from an earlier version that was used to study pion electroproduction. Some initial results are presented.

Radiative corrections are usually calculated using the formalism originally developed by Schwinger and Mo and Tsai [25, 26]. In that approach, it was assumed that only the scattered electron was detected (inclusive scattering). That method suffers from several shortcomings. First, detecting the ejected hadron (exclusive reactions) alters the phase space that is allowed for the final radiated photon. Second, more structure functions can contribute in exclusive reactions. Only the longitudinal and transverse pieces contribute in the Schwinger/Mo and Tsai method while for the out of plane production analyzed in this project there are components associated with the f_{LT} , f_{TT} and f'_{LT} structure functions. Third, the Schwinger/Mo and Tsai approach relies on an unphysical parameter to split the hard and soft regions of the radiated photon's phase space and cancel the infrared divergence. The method used here relies on a covariant procedure of infrared divergence cancellation which does not require the splitting [27].

These calculations are being done with a modified version of the computer program EXCLURAD written by Afanasev, *et al.* [28]. The code was originally written for the $p(e, e'\pi^+)X$ reaction and it has been modified to work for the $d(\vec{e}, e'p)n$ reaction. It includes processes that are left out of the Schwinger/Mo and Tsai approach including QED processes

for the undetected, radiated photon, vacuum polarization, and lepton-photon vertex corrections [28]. The program calculates the ratio of the cross section in a particular bin in Q^2 , W , $\cos\theta_{ps}^{cm}$, and ϕ_{pq} to the PWIA result.

The original pion electroproduction version of EXCLURAD has been modified for the $d(\vec{e}, e'p)n$ reaction by, first, modifying the masses of the target and final hadrons. Next, a new way to calculate the response functions is required. At this time the program DEEP is being used to calculate these response functions [29]. This code uses the covariant spectator theory and the transversity formalism to calculate the unpolarized, coincidence cross section for $d(\vec{e}, e'p)n$. Note, DEEP does not calculate the structure functions associated with polarized leptons, so there will be no cross section for out-of-plane hadrons. DEEP was modified from its original form so it could be called from a subroutine within EXCLURAD and its output was modified to be consistent with the formalism used by Afanasev, *et al.* in EXCLURAD.

More details on running the new code can be found in Reference [30]. Note that because of the adaptive stepsize used in performing some of the integrals in the code, the run time can vary from a few tens of seconds to several hours. The results shown below were performed on the computing cluster in my laboratory at the University of Richmond [31]. Figure 7 shows a comparison between the radiative corrections calculated with EXCLURAD versus a Schwinger calculation (black curve) over the Q^2 range of the E5 data set [32]. The Schwinger

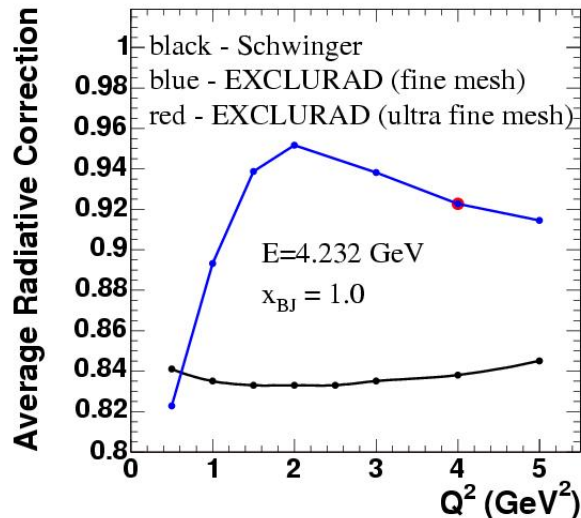


Figure 7: Comparison of radiative corrections calculated with the modified version of EXCLURAD for $d(\vec{e}, e'p)n$ and a Schwinger calculation.

calculation varies little across the Q^2 range while the EXCLURAD calculation (blue curve) changes by more than 10%. Radiative corrections for the exclusive reaction $d(\vec{e}, e'p)n$ using a more complete calculation of the response functions are significantly different than the Schwinger ones. The single red point at $Q^2 = 4.0$ (GeV/c)² is a calculation using a smaller stepsize to test the convergence of the EXCLURAD calculation.

One of the analyses being performed with the E5 data set is the measurement of the neutron magnetic form factor G_m^n using the ratio of the $d(e, e'p)n$ and the $d(e, e'n)p$ reactions

[33]. The expectation here is that by taking the ratio of these two reactions systematic uncertainties can be reduced or even eliminated. For the case of radiative corrections, that expectation has been tested using EXCLURAD and is shown in Figure 8. For the kinematics

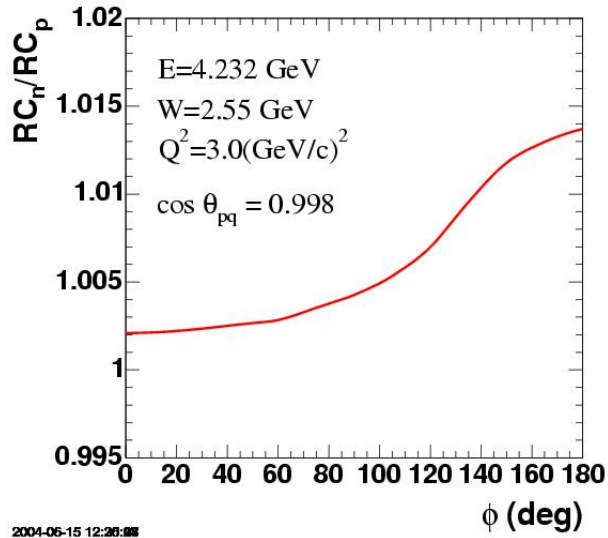


Figure 8: Ratio of radiative corrections for ep to en scattering.

shown, the red curve is the ratio of the radiative correction for the $d(e, e'n)p$ to the one for the $d(e, e'p)n$ reaction as a function of ϕ_{pq} . This ratio varies with the azimuthal angle, but never exceeds a 1.5% change from unity. This variation is well within the expected precision for the measurement.

2.2.2 Richmond Computing Cluster

A computing cluster has been built at the University of Richmond consisting of 53, 1.4-GHz, dual-CPU machines supported by 4.5 TByte of storage space. The cluster is used primarily for CLAS data analysis and simulation. The system was obtained with a National Science Foundation Major Research Instrumentation grant (\$150k) and University of Richmond funds (\$30k). The primary users of the system are my students and me, Dr. D.Jenkins from Virginia Tech, other members of the CLAS Collaboration (M.F.Vineyard, L.Todor, J.Lachniet) and several JLab accelerator staff. The machine arrived in February 2002 and has been used almost continuously since that time. It is worth noting here that the original machines are now showing signs of aging. Some of the ‘slave’ nodes no longer work and the fileserver which handles access to three, 1-TBytes, RAID disks that hold the data has failed. The fileserver is being replaced, but there are insufficient funds for replacing the broken slave nodes. A new ‘master’ node was recently purchased because the vendor’s experience has shown these machines’ active life is about 3 years. The system is described in more detail in Reference [31].

2.2.3 Online Monitoring

The CLAS is a large, complex detector that collects data at a prodigious rate so it is essential that the incoming data be carefully monitored to enable early detection of any problems. In CLAS there are two programs used for this purpose. One is `event_monitor` which does a comparatively simple analysis on a large fraction of the events in the data stream. It measures quantities such as the number of data words per event by sector, the number of data words in different detector components per event and by sector, *etc.* Another program is `recon_online` or online RECSIS which performs a full, time-consuming event reconstruction on a much smaller portion of the data stream. I am responsible for this second monitoring tool. The CLAS standard reconstruction code RECSIS has been modified to read data from the CLAS event transfer (ET) system so users can perform full-fledged track reconstruction and other complex analyses during data acquisition on a down-scaled subset of the incoming data. The capability of reading the ET system is part of the standard RECSIS so that users performing offline analyses can quickly and easily generate a version of their code that can be used during data collection. A number of histograms have been developed for monitoring purposes and these are used to generate timelines of various quantities that be observed using a web-based interface from anyplace on the internet. The code has been operating reliably for several years now. More details can be found in References [34, 35].

3 Task Description

In this section, the goals of my research efforts over the next three years will be mapped out. The primary focus will be on the analysis of the $d(\vec{e}, e'p)n$ reaction to extract the deuteron structure functions and on extending that analysis to higher Q^2 and ν . As part of that effort and my CLAS Collaboration service work I will continue to develop the program EXCLURAD for use in calculating radiative corrections for this reaction. I will also maintain the Richmond computing cluster (see Section 2.2.2) and online monitoring code described in Section 2.2.3.

3.1 Out-of-Plane Measurements of Deuteron Structure Functions

In this section I describe my plan for the analysis of the $d(\vec{e}, e'p)n$ reaction. The physics motivation is discussed first followed by a presentation of the existing data on this reaction and other experiments relevant to this investigation. New experimental directions are discussed.

3.1.1 Physics Motivation

Understanding the deuteron tests the ‘standard’ or hadronic model of nuclear physics. The goal is to construct a ‘consistent and exact description’ of few-body nuclei (^2H , ^3H , ^3He , ^4He) [4]. For example, it is an open question whether a single interaction or current operator can account for the attributes of all these nuclei. Calculations using hadronic effects like meson-exchange currents (MEC), isobar configurations (IC), and final-state interactions (FSI) are under development, but have yet to be fully challenged by data in the GeV region [4, 5]. The influence of relativity is also being studied [4, 5, 6, 7, 36]. Previous results at lower

Q^2 reveal the onset of many of these effects so a complete, modern calculation is needed to compare with data across the full range of Q^2 to test and understand the hadronic model in this region. These issues were raised as ‘Key Questions’ at the Jefferson Laboratory PAC14 Few-Body Workshop [4].

Of equal importance is finding where and how the hadronic model of nuclear physics breaks down; requiring quark-gluon or quark and flux-tube degrees-of-freedom. Studying this transition is an essential goal of nuclear physics as described by the JLab Physics Advisory Committee and the Nuclear Science Advisory Committee [3, 4]. The basic idea is that if we cannot describe observations with all of the pieces mentioned above, then we would see genuine quark effects in the nucleus. Clearly, we cannot make that leap without getting firm control of the calculations using the hadronic degrees-of-freedom. It is expected the transition may occur in the GeV region or higher and some expect the region $1 \text{ (GeV/c)}^2 < Q^2 < 6 \text{ (GeV/c)}^2$ to be an ideal one for investigating this transition [3, 5, 37].

Recent results imply two things. First, the boundary between the hadronic and quark regions is not simple [8, 9]. The workers in Reference [8] observed the onset of scaling (indicative of quark degrees of freedom) in deuteron photodisintegration, but only in certain angular regions. Second, discriminating between the two pictures is a serious challenge. A theoretical study by Thomas and Guichon starting with the quark-meson-coupling model revealed the NN force is similar to the NN force of the hadronic model [38]. This conclusion means we need probes sensitive to a broad range of physics effects across a wide kinematic range to see how the observations change and search for deviations from the hadronic picture. This work is a step in that direction. It will probe poorly known and even unknown parts of the deuteron wave function over a broad kinematic range with a consistent set of tools.

The mixture of physics effects that influence the different structure functions depends on the transferred energy in this energy region. For quasi-elastic scattering, FSI and relativistic corrections are important for f'_{LT} , but MEC and IC are less so [12]. For f_{LT} and quasi-elastic kinematics it appears that relativistic corrections are dominant. At higher energy transfer, *i.e.* in the dip region region, MEC and IC become important in f_{TT} while the influence of FSI and RC decline [11, 14]. Thus, a complete analysis of all these out-of-plane structure functions is necessary to unravel the deuteron’s electromagnetic response.

3.1.2 Existing Data and Related Experiments

Existing measurements of f'_{LT} are sparse. For quasi-elastic kinematics they have only been made at $Q^2 = 0.22 \text{ (GeV/c)}^2$ and $Q^2 = 0.13 \text{ (GeV/c)}^2$ at Bates [11, 12, 13]. An example of the results is shown in Figure 9. That work demonstrated the feasibility of out-of-plane measurements and the calculations show that relativity already plays a significant role even at this low value of Q^2 [36]. The effect of final-state interactions is dramatic and can be seen in the bottom panel of Figure 9. The double-dot-dashed line at $f'_{LT} = 0$ is from a Plane-Wave Born Approximation calculation which does not include FSI. In general, f'_{LT} is non-zero only in the presence of final-state interactions. The other calculations include FSI and they are all significantly different from zero. Unfortunately, the large uncertainties of the data prevent one from distinguishing among different effects like relativistic effects, MEC, FSI, and IC or between different potentials. Beyond quasi-elastic kinematics, there is a single measurement at $Q^2 = 0.15 \text{ (GeV/c)}^2$ in the dip region [14]. The results for f'_{LT}

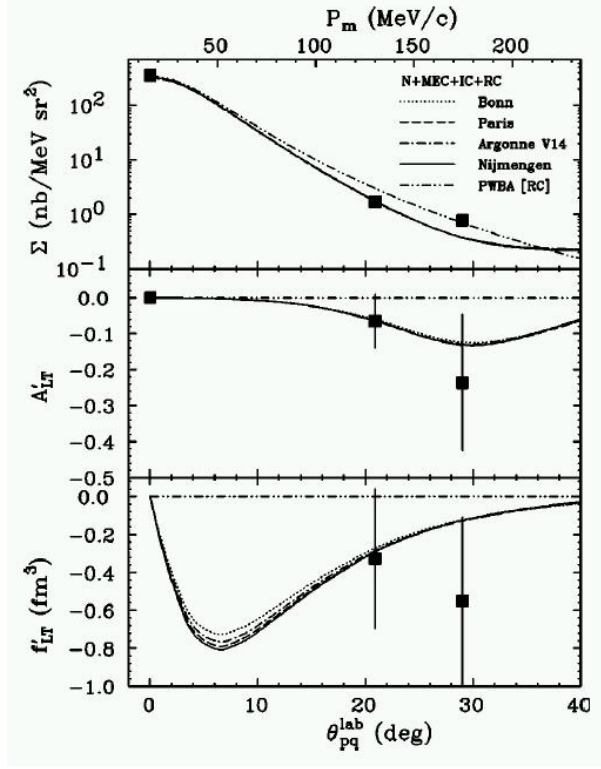


Figure 9: Measurements of f'_{LT} and its associated cross section and asymmetry from Reference [12] at $Q^2 = 0.13 \text{ (GeV/c)}^2$.

again reveal the importance of FSI, but limited statistics make further conclusions difficult. The success of the Bates work at low Q^2 is an invitation to extend the measurements with CLAS.

The situation is little different for observations of the transverse-transverse interference term f_{TT} . These experiments do not require out-of-plane measurements and polarized beams, but this portion of the cross section must be separated from the larger contributions of f_L , f_T , and f_{LT} . Three measurements in quasi-elastic kinematics have been made at Tohoku ($Q^2 = 0.013 \text{ (GeV/c)}^2$), NIKHEF ($Q^2 = 0.21 \text{ (GeV/c)}^2$), and Bates ($Q^2 = 0.22 \text{ (GeV/c)}^2$) [11, 39, 40]. The lowest Q^2 measurements agree with a non-relativistic calculation, but the uncertainties on all the data sets make it difficult to distinguish MEC, IC, FSI, and RC. There is a clear need here to reduce the uncertainties and extend the measurements out to larger θ_{pq}^{cm} where the calculations diverge. For dip kinematics, there is a single measurement at $Q^2 = 0.15 \text{ (GeV/c)}^2$ [14]. A calculation that included FSI, MEC, IC, and RC reproduced the limited data set.

The longitudinal-transverse interference structure function f_{LT} has been measured several times and with greater precision than the other two structure functions above. At the lowest $Q^2 = 0.013 \text{ (GeV/c)}^2$ the data are reproduced by a non-relativistic calculation while at the highest ($Q^2 = 1.2 \text{ (GeV/c)}^2$) the relativistic calculations of the asymmetry are preferred [39, 41]. Between these two extremes, the situation is less clear. For example, some calculations favor relativistic corrections [42] while others at nearby Q^2 favor a non-relativistic

calculation over a relativistic one [43, 44]. A recent JLab measurement supported inclusion of relativistic effects [45]. For dip kinematics at $Q^2 = 0.15 \text{ (GeV/c)}^2$ a calculation including FSI, MEC, IC, and RC reproduced the limited data set [14].

This analysis project will complement other experiments at Jefferson Lab. Experiment E02-101 (K. Wang spokesperson and contact) is designed to extract all the structure functions f_L , f_T , f_{LT} , f_{TT} , and f'_{LT} at threshold kinematics for $Q^2 = 0.47 \text{ (GeV/c)}^2$. Threshold kinematics have been chosen to minimize the contribution of nucleonic effects to study the effects of RC, MEC, and IC. The analysis project proposed here of quasi-elastic and dip kinematics explores different physics. In addition, E02-101 will take data at a single Q^2 while the CLAS data cover a larger kinematic region. Figure 3 displays a comparison of the kinematic coverage of E01-020 and this analysis.

Experiment E01-020 has two parts made up of two previous proposals: PR-01-007 (formerly E94-004, W.Boeglin spokesperson and contact) and PR-01-008 (P.Ulmer spokesperson and contact). Data collection for this experiment was completed in fall, 2002 in Hall A. In the first part (the former E94-004) parallel and anti-parallel kinematics will be used to study the short-range structure of the deuteron. Perpendicular kinematics at the quasi-elastic peak will be used to extract f_{LT} at $Q^2 = 0.8, 2.1, \text{ and } 3.5 \text{ (GeV/c)}^2$. The measurement of f_{LT} in this experiment overlaps with our proposed analysis project. However, we will be able to extract f_{TT} and f'_{LT} using our out-of-plane measurements. The CLAS detector has lower resolution, but greater kinematic coverage so the two experiments will provide a cross-check for each other. See Figure 3 for a comparison of the kinematics of E01-020 with this analysis.

In the second part of E01-020, the angular distribution of the quasi-elastic peak will be measured at the same values of Q^2 and with recoil momenta between 0.2 GeV/c and 0.5 GeV/c. The goal is to study FSI and non-nucleonic degrees of freedom (MEC and IC). The measurements will be entirely in the scattering plane. The kinematic region overlaps with the CLAS data of this proposed analysis, but no effort will be made to extract the structure functions.

3.1.3 Analysis Plan for E5 Data Set

In this section I map out a plan for the next three years and beyond. My primary focus is on the study of the deuteron structure functions measured using the out-of-plane production of the $d(\vec{e}, e'p)n$ reaction as a unique probe of the system. Much progress has already been made in the analysis of the E5 data and those results are discussed in Section 2.1 and Appendix C of this renewal application and in Reference [20].

The next phase of this project will be to complete the analysis of the A'_{LT} asymmetry for quasi-elastic kinematics in the E5 data set. We are now improving the data selection with more careful electron fiducial cuts and studying the effect of electron momentum corrections on the asymmetries. The results will be tested in a variety of ways including checks on the beam helicity (see Section 2.1.2), comparing overlaps between different run conditions, and others. Radiative corrections will be applied (see Section 2.2.1) and acceptance corrections will be calculated. The acceptance calculations are computationally intensive and will make use of the Richmond computing cluster. Uncertainties in the analysis will be studied and a comparison with theory made. We already have calculations from several theorists (H.A.Arenhövel, S.Jeschonnek, and J.W. Van Orden) and interest from others (J-M.Laget,

M.Sargsian).

Once this phase is done, the analysis of the fifth structure function and the asymmetry A'_{LT} will be extended from the quasi-elastic region to the dip region at higher energy transfer ν . As discussed in Section 3.1.1, the mix of physics effects changes as one moves away from the quasi-elastic region. In particular, meson-exchange current and isobar configurations become more important. This analysis will be very similar to the current work.

The next step is to extract the LT and TT structure functions in quasi-elastic kinematics. The asymmetries for this part of the deuteron structure functions are sensitive to different physics. For example, calculations of A_{TT} are more sensitive to IC at low Q^2 than A_{LT} or A'_{LT} . The analysis will be similar to the A'_{LT} work, but it will require a more careful acceptance calculation. Recall the conventional definitions of A_{LT} and A_{TT} in Equations 4-6. These asymmetries are equivalent to measurements at different ϕ_{pq} where the acceptance may be different. The last phase of the analysis on the E5 data will be to extend the work on A_{LT} and A_{TT} to the dip region at higher energy transfer. The LT part is less sensitive to FSI at low p_m (or low θ_{pq}^{cm}) in these kinematics and more sensitive to relativistic effects [11]. The TT part is effected by MEC and IC, but not FSI and relativistic effects [11].

3.1.4 New Experiments and Analyses

The goal of this research program is to study the transition from the hadronic picture of matter to the quark-gluon one. The analysis has begun of the deuteron structure functions below the 1 GeV region where we expect the hadronic picture to still hold. The natural extension of this program is to go to higher Q^2 . There are already existing data sets and planned experiments that may accomplish at least part of this goal. It is expected by some that this region(where $1 (\text{GeV}/c)^2 < Q^2 < 6 (\text{GeV}/c)^2$) may be the best place to see and understand the transition to quark degrees of freedom [37].

The relevant experiments are summarized in Table 1. The name of the running period is listed in the first column followed by the beam energies used, the number of electron events from the deuterium target, and finally the status. The first-pass analysis of the data is done on the JLab computing farm and further analysis is done on the Richmond cluster. I am now analyzing the E5 data set which collected data at two beam energies (4.2 GeV and 2.6 GeV) and included reversed field running at 2.6 GeV to reach lower Q^2 (below $1 (\text{GeV}/c)^2$). This last feature is important because this region of Q^2 is where the hadronic picture is valid. The E6 running period is at higher energy and Q^2 so extracting the structure functions from those data pushes into the region where the transition to quark-gluon degrees of freedom may become relevant. The EG1 period used a series of beam energies and a polarized target so the analysis described here does not directly apply. The EG2 running period was completed last summer, but did not collect the beam helicity information necessary for the fifth structure function (f'_{LT}) analysis.

The last entry in Table 1 is for an approved, but not yet scheduled, CLAS experiment, E02-012, to study vector meson production off deuterium. This experiment will run at high energy (6 GeV) and more importantly at higher luminosity. This higher luminosity means this experiment will acquire about 10 times the amount of data as the E6 experiment (second entry in Table 1). This experiment will significantly improve the precision of the measurements. E02-012 received a high grade A⁻ from the JLab PAC and I have already

Run Period	Run Conditions	Deuterium Triggers	Status
E5	2,4 GeV	2×10^9	First-pass analysis complete.
E6	6 GeV	4×10^9	First-pass analysis complete.
EG1	1.6 - 5.7 GeV	9×10^9	First-pass analysis complete, polarized target.
EG2	4 and 5 GeV	3×10^9	Recently completed, no helicity information.
E02-012	6 GeV	40×10^9	Approved, not yet scheduled.

Table 1: Listing of JLab run periods and approved experiments using a deuterium target. The last entry is for an approved experiment that has not yet run.

begun working with the collaboration involved in this experiment.

In April 2004, JLab received approval from the Department of Energy to begin work to upgrade the accelerator and end stations to reach higher energies. The higher energies and 4-momentum transfers available with the upgraded facilities will be where quark and gluon effects should be significant. Measuring the structure functions up to a beam energy of 11 GeV and Q^2 of 14 $(\text{GeV}/c)^2$ (the maximum beam energy and momentum transfer that will be available in Hall B) will complete a single, consistent data set that begins where the hadronic model applies and extends to where the quark-gluon picture will be the correct one. My initial studies of this higher energy and Q^2 show that the cross section drops by a factor of 10-20 [21]. However, the CLAS detector will be upgraded (and dubbed CLAS++) so that it can handle a luminosity that is ten times the current limit. The drop in cross section (and count rate) will be roughly canceled by the increase in luminosity. I have also found the asymmetry ratio A'_{LT} actually increases at these higher energies. Another benefit of the JLab upgrade will be that the acceptance near $Q^2 \approx 6 (\text{GeV}/c)^2$ will increase making measurements more accessible in this important region [37].

3.2 CLAS Collaboration Service

My Collaboration service plan for the next three years is to continue work on radiative corrections for exclusive reactions on the deuteron, develop and maintain the Richmond computing cluster for use by CLAS Collaboration members (including me), and to maintain online RECSIS, one of the CLAS data-acquisition monitoring tools. This will be in addition to normal collaboration duties (taking shifts, reviewing papers and analyses, *etc.*).

I have modified the radiative correction program EXCLURAD for the $d(\vec{e}, e'p)n$ case. See Section 2.2.1 for more details. In the current version the deuteron response functions are calculated using the code DEEP from J.W.Van Orden [29] which does not include final-state interactions. I now have a copy of another program by S.Jeschonnek that uses an approach similar to the one in Reference [29], but has final-state interactions included. The code compiles and runs at Richmond. The next step is to modify the program so it can be called as a subroutine and then to merge it in EXCLURAD. The website describing the deuteron

version of EXCLURAD will be maintained and updated and an internal report (CLAS Note) is in preparation [30].

I maintain a 53-node, 106-CPU, 4.5-TByte computing cluster in my laboratory at the University of Richmond. See Section 2.2.2 and Reference [31] for more details. This instrument is used by several other CLAS Collaborators and me. See Appendix B for a list of collaborators and projects. I will continue to keep this system running and in this renewal application I request funds to replace some of the aging nodes to maintain the productivity of my work and the work of my CLAS collaborators.

Online RECSIS is a version of the CLAS standard analysis code RECSIS that includes the capability to read data from the incoming data stream during an experiment and do a full event reconstruction [34, 35]. Periodically during data acquisition some of the results from this reconstruction (*e.g.*, number of tracks per event, number of hits per event, *etc.*) are written to a database which can be accessed via the Internet so collaborators can monitor the progress of the experiment in the counting house, in their office, and even at home. I will continue to maintain this code and upgrade it in response to user requests.

3.3 Enhancement of Computing Facilities

I have developed a supercomputing cluster for data analysis and simulation to support the physics program in Hall B at Jefferson Lab. In this section I describe the existing computing facility and propose a replacement plan for the future to improve the cluster performance and enhance our research productivity. Maintaining this facility at Richmond improves the scientific productivity of the system's users (including me) and it relieves pressure on the computing farm at JLab. A description of the outside user projects is in Appendix B.

The supercomputing cluster is used for two primary tasks: analysis of 'cooked' data from CLAS (including radiative corrections) and simulation of the CLAS response. Cooked data is the result of the first-pass analysis to produce data summary tapes and is performed at JLab. The analysis of this first-pass data still requires considerable computing power and storage space. For example, the first-pass data for the E5 running period occupies about 0.8 TByte of space. To calculate radiative corrections for E5 (see Section 2.2.1) the program EXCLURAD is used for exclusive reactions like the $d(\vec{e}, e'p)n$ one here. This algorithm performs some computer-intensive integrations that require up to 20 CPU-hours on each node of the Richmond cluster to cover the full range of kinematics for a single set of running conditions. Such a calculation would take many weeks on a single machine. The simulation of the CLAS for analysis testing and acceptance calculations is another essential part of this program. Acceptance calculations require days to weeks even on the Richmond cluster.

The current system is summarized in the table below. Most of it was purchased with a \$175,000 Major Research Instrumentation grant from the National Science Foundation along with some matching funds from the University. The system was installed in February, 2002 and consists of 53, dual-processor machines with 256 MByte RAM for each processor and a 20-GByte disk. A 3.3-TByte disk array provides additional storage.

I propose here to improve the performance of the cluster over the next three years by gradually adding newer, more capable machines. During the summer of 2004, several machines failed for various reasons. This was initially surprising, but consistent with the experience in the Computer Center at JLab where they maintain a 200-node computing farm.

Component	Description	number
Processors	1.4 GHz Pentium 4	106
Memory	256-MByte RAM	106
Storage	20-GByte disk	53
	3.3-TByte disk array	1

Table 2: Summary of the components of the computing cluster at the University of Richmond.

At JLab they have a policy where machines that develop problems when they are more than 2-1/2 years old are replaced and all machines are replaced by the time they are four years old. Computers in the farm simply live shorter lives than desktop machines because of the intense demands of scientific computing. They even put identical machines in the farm and on desktops and the farm machines failed much sooner than the desktop ones. This lifetime is also consistent with the experience of our vendor. The computers in the Richmond cluster will be three years old in February, 2005.

Replacing these machines is a good investment. The infrastructure is already in a place to make efficient use of the new machines. To support the NSF MRI grant the University built a new, 600 ft² lab for the cluster with a 5-ton air conditioning unit and additional power. The cluster laboratory has the necessary disk storage, high-speed switch (for communicating among the nodes), racks, backup power, and a high-speed network connection. The software and associated documentation for using the cluster has been developed and thoroughly tested [31]. About two years ago the University hired its first linux support person who has provided invaluable assistance in maintaining the current cluster. More importantly, there is a community of users (besides me) that use the system. See Appendix B for short descriptions of the projects being performed by users from the CLAS Collaboration, but outside the University of Richmond. The Richmond cluster is often more accessible than the one at JLab where the demand is higher. Remember the first-pass analysis (cooking) is done at JLab. Finally, this investment will take advantage of the improving price-to-performance ratio of modern computers. In 2002, the compute nodes cost about \$2,900 per 1.4-GHz, dual-processor computer. A replacement machine from the same vendor costs almost exactly the same amount (\$2,879, see quote in Appendix A) for a 3.1-GHz, dual-processor with twice as much memory. The proposal here is to obtain six new machines each year for the next three years (2005-2007). With the continuing increase in computing power these 18 new machines will replace the computing power of many more older machines that will be out of service by that time. Maintaining the computing power of the cluster will enable the users to maintain their scientific productivity.

3.4 Institutional Support and Resources

The University of Richmond, established in 1830, is one of America's premier private, highly selective, independent liberal arts universities. The University promotes high academic standards, core values and technological expertise among its students. It is primarily an under-

graduate liberal arts institution. The undergraduate population is approximately 3,000 (51% women, 49% men; 13% minority), with outstanding students from nearly every state and about 70 foreign countries. Out of 5,899 applications for Fall 2002, 782 matriculated; entering students had average SAT scores in the 1240-1370 range.

The University of Richmond completed a campus-wide strategic planning process in 2000. The Science Initiative is the highest priority in the strategic plan, and includes a comprehensive upgrade of the science facilities and curriculum, intended to make Richmond the first choice college of the best students in America. Over the next ten years, there will be a \$35 million renovation of the Gottwald Science Center, and more than \$60 million will be devoted to program enhancements.

The University has provided support for the project described in this renewal application over the last three years. It provided about \$24,000 in matching funds for the NSF Major Research Instrumentation grant to support the original purchase of the Richmond computing cluster and added about \$6,000 later to obtain three additional compute nodes. Each summer the University supports about 20 undergraduates in all disciplines with summer stipends to do research with faculty. One of my students, Arthur Rayner, received such a stipend during the summer of 2003. This additional support enabled me to hire three students last summer (2004). The University also provides some travel support for students to attend conferences. My students have received about \$2,500 in travel support over the last three years. Finally, two years ago the University hired the first technical support person with Linux experience on its information services staff (the computing cluster uses the Linux operating system). This technical support person has provided help with routine backups, software upgrades, and set up the current firewall to make the cluster more secure [46].

3.5 Education of Students

Undergraduates have been involved in all the stages of the physics program described in this renewal application and the funds requested here will enable me to provide an intense summer research experience for these young people. The environment at Richmond is an ideal one for undergraduates to learn the joys and rigors of scientific research and I have been successful at attracting students into physics and encouraging them to go further into scientific and technical careers. Since my arrival at Richmond in 1987 I have averaged 2-3 undergraduates doing research with me every summer. About two-thirds of the students have gone on to graduate school in physics, computer science, chemistry, or engineering. Some of the schools they have attended include the University of California at Santa Barbara, the University of Virginia, the University of North Carolina, Virginia Tech, Princeton, Harvard, the University of Pittsburgh, and the University of Alabama-Huntsville. Five former students from my laboratory have received doctorates. Three are currently staff scientists at NASA-Goddard, NASA-Huntsville, and the Jet Propulsion Laboratory (JPL), one is a faculty member at Stanford, and one is a post-doctoral fellow at the University of Chicago in high-energy physics. Several others are practicing engineers and one is a local high school science teacher.

The students who work in my laboratory use the supercomputing cluster to perform data analysis, radiative corrections, and Monte-Carlo simulations. They travel to JLab to take shifts with me and attend CLAS Collaboration meetings. They learn nuclear physics

and modern scientific computing methods including hardware and software installation and maintenance, and computer security. For several years now I have used computer science undergraduates to do maintenance work and testing on the cluster [46, 47]. One of these students is now in graduate school in computer science while two others have gone into industry. All of my students are strongly encouraged to present their work at local, national, and international conferences [46, 47, 48, 49]. One student, Arthur Rayner, has worked for me during each of the last three summers and has given talks at the National Conference on Undergraduate Research (in Salt Lake City) and at the International Conference in Physics Students (in Denmark) [48, 49]. The continued funding of this program will enable me to provide meaningful research experiences for many more undergraduate students.

References

- [1] B. Mecking, *et al.*, Nucl. Inst. and Methods in Physics Research, **A503/3**, 513 - 553, (2003); W.K. Brooks, Nucl. Phys. **A663-664**, 1077 (2000).
- [2] See the publications list on the Hall B website at <http://www.jlab.org/Hall-B/pubs/>, last accessed Nov. 15, 2004.
- [3] ‘Opportunities in Nuclear Science: A Long-Range Plan for the Next Decade’, DOE/NSF Nuclear Science Advisory Committee, April 2002, p. 30.
- [4] PAC 14 Few-Body Workshop, Williamsburg, VA, July, 1998.
- [5] S.Jeschonnek, Phys. Rev **C63** 034609 (2001).
- [6] S.Jeschonnek and T.W.Donnely, Phys. Rev. **C57** 2438 (1998).
- [7] S.Jeschonnek and J.W.Van Orden, Phys. Rev. **C62** 044613 (2000).
- [8] P.Rossi, *et al.* (the CLAS Collaboration), ‘Onset of asymptotic scaling in deuteron photodisintegration’, accepted for publication in Phys. Rev. Lett.
- [9] R.Gilman, ‘Experimental Signatures of the Limits of the Hadronic Description of Nuclei’, presented at the Workshop on Physics of Nuclei at 12 GeV, Jefferson Lab, Newport News, Va, Nov 2, 2004.
- [10] S. Boffi, C. Giusti, F. D. Pacati, and M. Radici, *Electromagnetic Response of Atomic Nuclei*, Oxford University Press, Oxford, England, 1996.
- [11] S.Gilad, W.Bertozzi, and Z.-L.Zhou, Nucl. Phys. **A631** 276c (1998).
- [12] S.M.Dolfini *et al.*, Phys. Rev. **C60** 064622 (1999).
- [13] S.M.Dolfini, *et al.*, Phys. Rev. **C51** 3479 (1995).
- [14] Z.-L. Zhou *et al.*, Phys. Rev. Lett. **87** 172301 (2001).
- [15] K.Joo, C.Smith, *et al.* (the CLAS Collaboration), Phys. Rev. C, **68**, 032201 (2003).

- [16] A. Klimenko and S. Kuhn, CLAS-Note 03-005.
- [17] K. Park, V. Burkert, L. Elouadrhiri, W. Kim, CLAS-Note 03-012.
- [18] D. Protopopescu, F.W. Hersman, M. Holtrop, S. Stepanyan, CLAS-Note 01-008.
- [19] K. Y. Kim, H. Denizli, J. A. Mueller, S. A. Dytman, CLAS-Note 01-018.
- [20] G.P.Gilfoyle, W.K.Brooks, B.A.Mecking, S.Kuhn, L.Weinstein, and M.F.Vineyard, CLAS Approved Analysis, G.P. Gilfoyle, (Spokesperson), Nov 2003, http://www.richmond.edu/~ggilfoyl/research/eod/deuteron_electrodisintegration.ps, [Last accessed Nov 15, 2004].
- [21] S.Jeschonnek, private communication.
- [22] H.Arenhövel, private communication.
- [23] K.Joo, private communication.
- [24] J.Lachniet, B.P.Quinn, private communication.
- [25] J.Schwinger, Phys. Rev., **76**, 898, 1949.
- [26] L.W.Mo and Y.S.Tsai, Rev. Mod. Phys., **41**, 205, 1969.
- [27] D.Y.Bardin and N.M.Shumeiko, Nucl. Phys. B, **127**, 242 (1977).
- [28] A.Afanasev, I.Akushevich, V.Burkert, and K.Joo, Phys.Rev., **D66**, 074004, 2002.
- [29] J.Adam, Jr., F.Gross, S.Jeschonnek, P.Ulmer, and J.W. Van Orden, Phys. Rev. C, **66**, 044003 (2002).
- [30] G.P.Gilfoyle and A.Afanasev, CLAS Note in preparation; G.P.Gilfoyle, ‘Radiative Corrections Using Deep’, <http://www.richmond.edu/~ggilfoyl/research/RC/wvo.html>, [Last accessed Nov 15, 2004].
- [31] G.P.Gilfoyle, ‘The Richmond Computing Clusters’, http://www.richmond.edu/~ggilfoyl/research/spiderwulf/cluster_home.html, [Last accessed Nov 15, 2004].
- [32] Juan Cornejo, *radiative corrections, external and internal bremsstrahlung factors*, Retrieved on January 30, 2003 from http://www.calstatela.edu/academic/nuclear_physics/schwin12.extbrems.html.
- [33] W.K.Brooks and M.F.Vineyard, ‘The Neutron Magnetic Form Factor from Precision Measurements of the Ratio of Quasielastic Electron-Neutron to Electron-Proton Scattering in Deuterium’, Jefferson Lab experiment E94-017.
- [34] G.P.Gilfoyle, ‘Using the Online Version of RECSIS’, http://www.jlab.org/~gilfoyle/reccsis_online/reccsis_online.html, [Last accessed Nov 15, 2004].

- [35] G.P.Gilfoyle, M.Ito, and E.J.Wolin, ‘Online RECSIS’, CLAS-Note 98-017.
- [36] F.Ritz, H.Goller, Th. Wilbois, and H.Arenhövel, Phys. Rev. **C55**, 2214 (1997).
- [37] M.Sargsian, Int. J. Mod. Phys., E10:405-458 (2001).
- [38] A.W.Thomas and P.A.M.Guichon, Phys. Rev. Lett., **93**, 132502 (2004),
- [39] T.Tamae, *et al.*, Phys. Rev. Lett. **59** 2919 (1987).
- [40] M. van der Schaar *et al.*, Phys. Rev. Lett. **68**, 776 (1992).
- [41] H.J.Bulten, *et al.*, Phys. Rev. Lett. **74** 4775 (1995).
- [42] E.Hummel and J.A.Tjon, Phys. Rev. Lett. **63**, 1788 (1989); Phys. Rev. **C42** 423, (1990).
- [43] D.Jordan *et al.*, Phys. Rev. Lett. **76** 1579 (1996).
- [44] J.E.Ducret, *et al.*, Phys. Rev. **C49** 1783 (1994).
- [45] P.E.Ulmer, *et al.*, Phys. Rev. Lett. **89**, 062301, 2002.
- [46] V.Davda* and G.P.Gilfoyle, ‘Maintenance and Upgrading of the Richmond Physics Supercomputing Cluster’, poster presented at the Conference Experience for Undergraduates at the Fall 2003 Meeting of the Division of Nuclear Physics of the American Physical Society, Tucson, AZ, Oct 30 - Nov 1, 2003.
- [47] F. Chinchilla*, M.S. Fetea, G.P. Gilfoyle, and M.F. Vineyard, ‘From Quarks to Nucleons’, 14th Summer School on Understanding the Structure of Hadrons, Prague, Czech Republic, July 9-13, 2001.
- [48] A. Rayner*, and G.P.Gilfoyle, ‘Pion Identification in CLAS’, Program and Abstracts of the Conference of the International Association of Physics Students, Odense, Denmark, August 14, 2003.
- [49] A. Rayner*, A.Mackenzie*, and G.P.Gilfoyle, ‘Pion Identification in CLAS’, Program and Abstracts of the Seventeenth National Conference on Undergraduate Research, University of Utah, UT, March 13-15, 2003.

Contract-Related Refereed Publications (2001-2004)

1. M. Miraziti, *et al.* (The CLAS Collaboration), ‘Complete Angular Distribution Measurements of Two-Body Deuteron Photodisintegration between 0.5 and 3 GeV’, *Physical Review C* **70**, 014005 (2004).
2. K. McCormick, *et al.* (The CLAS Collaboration), ‘Tensor Polarization of the phi meson Photoproduced at High t' ’, *Physical Review C* **69**, 032001 (2004).
3. V. Kubarovsky, L. Guo, *et al.* (The CLAS Collaboration), ‘Observation of an exotic baryon with $S=+1$ in photoproduction from the proton’, *Physical Review Letters* **69**, 032203 (2004).
4. R. Niyazov, *et al.*, (The CLAS Collaboration), ‘Two-Nucleon Momentum Distributions Measured in ${}^3\text{He}(e, e'pp)n$ ’, *Phys. Rev. Lett.* **92**, 052303 (2004).
5. S. Stepanyan, *et al.* (The CLAS Collaboration), ‘Observation of an Exotic $S = +1$ Baryon in Exclusive Photoproduction from the Deuteron’, *Physical Review Letters* **91**, 252001 (2003).
6. R. Fatemi, *et al.*, (The CLAS Collaboration), ‘Measurement of the Spin Structure Functions in the Resonance Region for Q^2 from 0.15 to 1.6 GeV^2 ’, *Phys. Rev. Lett.* **91**, 222002 (2003).
7. K. Joo, *et al.* (The CLAS Collaboration), ‘Measurement of Polarized Structure Function $\sigma(LT')$ for $p(\vec{e}, e'p)\pi^0$ from single π^0 electroproduction in the Delta resonance region’, *Physical Review C, Rapid Communications*, **68**, 032201 (2003).
8. B. Mecking, *et al.*, (The CLAS Collaboration), ‘The CEBAF Large Acceptance Spectrometer’, *Nucl. Instr. and Meth.*, **503/3**, 513 (2003).
9. A. Biselli, *et al.*, (The CLAS Collaboration), ‘Study of the Delta(1232) using single and double polarization asymmetries’, *Phys. Rev. C* **68**, 035202 (2003).
10. K. Sh. Egiyan, *et al.* (The CLAS Collaboration), ‘Observation of Nuclear Scaling in the $A(e, e')$ Reaction at $x_B > 1$ ’, *Phys. Rev. C* **68**, 014313, (2003).
11. M. Ripani, *et al.*, (The CLAS Collaboration), ‘Measurement of $ep \rightarrow e'p\pi^+\pi^-$ and baryon resonance analysis’, *Phys. Rev. Lett.* **91** 022002, (2003).
12. J. Yun, *et al.* (The CLAS Collaboration), ‘Measurement of Inclusive Spin Structure Functions of the Deuteron with CLAS’, *Phys. Rev. C*, **67**, 055204 (2003).
13. D. Carman, *et al.*, (The CLAS Collaboration), ‘First Measurement of Transferred Polarization in the Exclusive $e(\text{pol})p \rightarrow e'K^+\Lambda(\text{pol})$ Reaction’, *Phys. Rev. Lett.* **90** 131804 (2003).
14. B. Mecking, *et al.*, (The CLAS Collaboration), ‘The CEBAF Large Acceptance Spectrometer’, *Nucl. Instr. and Meth.*, **503/3**, 513 (2003).

15. M. Osipenko, *et al.*, (The CLAS Collaboration), ‘A Complete Measurement of the F2 Proton Structure Function in the Resonance Region and the Evaluation of the Moments’, *Physical Review D* **67**, 092001 (2003).
16. M.Battaglieri, *et al.*, (The CLAS Collaboration), ‘Photoproduction of the Omega Meson at Large Momentum Transfer’, *Phys. Rev. Lett.* **90**, 022002 (2003).
17. M. Dugger, *et al.*, (The CLAS Collaboration), ‘Eta photoproduction on the proton for photon energies from 0.75 to 1.95 GeV’, *Phys. Rev. Lett.* **89**, 222002 (2002).
18. R. DeVita, *et al.*, (The CLAS Collaboration), ‘First Measurement of the Double Spin Asymmetry in $e(pol)p(pol) \rightarrow e'\pi^+n$ in the Resonance Region’, *Phys. Rev. Lett.* **88**, 082001 (2002).
19. K.Joo, *et al.*, (The CLAS Collaboration), ‘ Q^2 Dependence of Quadrupole Strength in $\gamma^*p \rightarrow \Delta^+(1232) \rightarrow p\pi^0$ Transition’, *Phys.Rev.Lett.* **88**, 122001 (2002).
20. G.P.Gilfoyle and J.A.Parmentola, ‘Using Nuclear Materials to Prevent Nuclear Proliferation’, *Science and Global Security* **9**, 81 (2001).
21. S. Stepanyan, *et al.* (The CLAS Collaboration), ‘First observation of exclusive DVCS in polarized electron beam asymmetry measurements’, *Phys.Rev.Lett.* **87**, 182002 (2001).
22. M.Battaglieri, *et al.*, (The CLAS Collaboration), ‘Photoproduction of ρ_0 Meson on the Proton at Large Momentum Transfer’, *Phys.Rev.Lett.* **87**, 172002 (2001).
23. S. Barrow, *et al.*, (The CLAS Collaboration), ‘Electroproduction of the Lambda(1520) Hyperon’, *Phys. Rev.* **C64**, 044601 (2001).
24. K. Lukashin, *et al.*, (The CLAS Collaboration), ‘Exclusive electroproduction of phi mesons at 4.2 GeV’ *Phys. Rev.* **C63**, (2001), 065205-1.
25. M.Kaplan, C.J.Copi, P.A.DeYoung, G.P.Gilfoyle, P.J.Karol, D.J.Moses, W.E.Parker, K.E.Rehm, J. Sarafa, and E.Vardaci, ‘Studies of light charged particle emission from fission and ER reactions in the system 344-MeV $^{28}\text{Si} + ^{121}\text{Sb} \rightarrow ^{149}\text{Tb}$ ($E^* = 240\text{MeV}$), *Nucl. Phys.* **A686**, 109 (2001).
26. R. Thompson, *et al.* (The CLAS Collaboration), ‘The $ep \rightarrow e'p(\eta)$ reaction at and above the S11(1535) baryon resonance’, *Phys. Rev. Letters* **86**, 1702 (2001).

Collaborating Institutions

The list below represents all the institutions that have members in the CLAS Collaboration.

1. Arizona State University, Tempe, Arizona 85287-1504
2. University of California at Los Angeles, Los Angeles, California 90095-1547
3. Carnegie Mellon University, Pittsburgh, Pennsylvania 15213
4. Catholic University of America, Washington, D.C. 20064
5. CEA-Saclay, Service de Physique Nucléaire, F91191 Gif-sur-Yvette, Cedex, France
6. Christopher Newport University, Newport News, Virginia 23606
7. University of Connecticut, Storrs, Connecticut 06269
8. Edinburgh University, Edinburgh EH9 3JZ, United Kingdom
9. Emmy-Noether Foundation, Germany
10. Florida International University, Miami, Florida 33199
11. Florida State University, Tallahassee, Florida 32306
12. The George Washington University, Washington, DC 20052
13. University of Glasgow, Glasgow G12 8QQ, United Kingdom
14. Idaho State University, Pocatello, Idaho 83209
15. INFN, Laboratori Nazionali di Frascati, Frascati, Italy
16. INFN, Sezione di Genova, 16146 Genova, Italy
17. Institut de Physique Nucleaire ORSAY, Orsay, France
18. Institute für Strahlen und Kernphysik, Universität Bonn, Germany
19. Institute of Theoretical and Experimental Physics, Moscow, 117259, Russia
20. James Madison University, Harrisonburg, Virginia 22807
21. Kyungpook National University, Daegu 702-701, South Korea
22. University of Massachusetts, Amherst, Massachusetts 01003
23. Moscow State University, General Nuclear Physics Institute, 119899 Moscow, Russia
24. University of New Hampshire, Durham, New Hampshire 03824-3568
25. Norfolk State University, Norfolk, Virginia 23504

26. Ohio University, Athens, Ohio 45701
27. Old Dominion University, Norfolk, Virginia 23529
28. University of Pittsburgh, Pittsburgh, Pennsylvania 15260
29. Rensselaer Polytechnic Institute, Troy, New York 12180-3590
30. Rice University, Houston, Texas 77005-1892
31. University of Richmond, Richmond, Virginia 23173
32. University of South Carolina, Columbia, South Carolina 29208
33. Thomas Jefferson National Accelerator Facility, Newport News, Virginia 23606
34. Union College, Schenectady, NY 12308
35. Virginia Polytechnic Institute and State University, Blacksburg, Virginia 24061-0435
36. University of Virginia, Charlottesville, Virginia 22901
37. College of William and Mary, Williamsburg, Virginia 23187-8795
38. Yerevan Physics Institute, 375036 Yerevan, Armenia

Dr. Gerard P. Gilfoyle

Physics Department
University of Richmond, VA 23173
ggilfoyl@richmond.edu

3234 Kensington Avenue
Richmond, VA 23221
804-289-8255

- Degrees** Ph.D., University of Pennsylvania, 1985 - 'Resonant Structure in $^{13}\text{C}(^{13}\text{C}, ^4\text{He})^{22}\text{Ne}$ ',
H.T. Fortune, advisor.
A.B., cum laude, Franklin and Marshall College, 1979.
- Experience** 2004-present - Professor of Physics, University of Richmond.
2002-2003 - Scientific Consultant, Jefferson Laboratory.
1999-2000 - Defense Policy Fellow, AAAS.
1994-1995 - Scientific Consultant, Jefferson Laboratory.
1993-2004 - Associate Professor of Physics, University of Richmond.
Summer, 1988 - Visiting Research Professor, University of Pennsylvania.
1987-1993 - Assistant Professor, University of Richmond.
1985-1987 - Postdoctoral Research Fellow, SUNY at Stony Brook.
1979-1985 - Research Assistant, University of Pennsylvania.
- Research and Teaching Grants** 2002-2003 - SURA Sabbatical Support (\$10,000).
2002-2003 - Jefferson Laboratory Sabbatical Support (\$28,335).
2002-present - Department of Energy (\$225,000).
2001-2002 - National Science Foundation (\$175,000).
1999-2002 - Department of Energy (\$222,000).
1996-1999 - Department of Energy (\$300,000).
1995-1997 - National Science Foundation(\$14,986).
1994-1995 - CEBAF Sabbatical Support (\$24,200)
1993-1996 - Department of Energy (\$284,000).
1992-1995 - National Science Foundation (\$49,813).
1990-1993 - Department of Energy (\$287,000).
1989-1991 - Research Corporation(\$26,000).
1987-2002 - University of Richmond Research Grants(\$13,082).
- Selected Service** 2003-present - Southeastern Universities Research Association Trustee.
2002-present - Reviewer, CLAS Collaboration.
2002 - Reviewer, Civilian Research and Development Foundation.
2002-2003 - American Physical Society Task Force on Countering Terrorism.
2000-present - Chair, Department of Physics.
2000 - Reviewer, US Department of Defense.
1999 - Reviewer, Department of Energy EPSCoR Program.
1997 - Chair, Jefferson Laboratory CLAS Collaboration nominating committee.
1996 - Chair, review panel, National Science Foundation, ILI Program.
1996-1998 - Managed the Physics Department's high school outreach program.
- Honors** 2003 University of Richmond Distinguished Educator Award.

Selected Refereed Publications (2001-2004)

1. M. Miraziti, *et al.* (The CLAS Collaboration), ‘Complete Angular Distribution Measurements of Two-Body Deuteron Photodisintegration between 0.5 and 3 GeV’, *Physical Review C* **70**, 014005 (2004).
2. V. Kubarovsky, L. Guo, *et al.* (The CLAS Collaboration), ‘Observation of an exotic baryon with $S=+1$ in photoproduction from the proton’, *Physical Review Letters* **69**, 032203 (2004).
3. R. Niyazov, *et al.*, (The CLAS Collaboration), ‘Two-Nucleon Momentum Distributions Measured in ${}^3\text{He}(e, e'pp)n$ ’, *Phys. Rev. Lett.* **92**, 052303 (2004).
4. S. Stepanyan, *et al.* (The CLAS Collaboration), ‘Observation of an Exotic $S = +1$ Baryon in Exclusive Photoproduction from the Deuteron’, *Physical Review Letters* **91**, 252001 (2003).
5. K. Joo, *et al.* (The CLAS Collaboration), ‘Measurement of Polarized Structure Function $\sigma(LT')$ for $p(\vec{e}, e'p)\pi^0$ from single π^0 electroproduction in the Delta resonance region’, *Physical Review C, Rapid Communications*, **68**, 032201 (2003).
6. B. Mecking, *et al.*, (The CLAS Collaboration), ‘The CEBAF Large Acceptance Spectrometer’, *Nucl. Instr. and Meth.*, **503/3**, 513 (2003).
7. K. Sh. Egiyan, *et al.* (The CLAS Collaboration), ‘Observation of Nuclear Scaling in the $A(e, e')$ Reaction at $x_B > 1$ ’, *Phys. Rev. C* **68**, 014313, (2003).
8. B. Mecking, *et al.*, (The CLAS Collaboration), ‘The CEBAF Large Acceptance Spectrometer’, *Nucl. Instr. and Meth.*, **503/3**, 513 (2003).
9. K.Joo, *et al.*, (The CLAS Collaboration), ‘ Q^2 Dependence of Quadrupole Strength in $\gamma^*p \rightarrow \Delta^+(1232) \rightarrow p\pi^0$ Transition’, *Phys.Rev.Lett.* **88**, 122001 (2002).
10. S. Stepanyan, *et al.* (The CLAS Collaboration), ‘First observation of exclusive DVCS in polarized electron beam asymmetry measurements’, *Phys.Rev.Lett.* **87**, 182002 (2001).

Other Selected Publications and Presentations (2001-2004)

1. ”Radiative Corrections for E5”, CLAS Collaboration Meeting, June 20, 2004.
2. ”Out-of-Plane Measurements of the Structure Functions of the Deuteron”, plenary session of the CLAS Collaboration Meeting, November 13, 2003.
3. G.P.Gilfoyle, ‘Swarm Intelligence’, *APS News*, January, 2003, published by the American Physical Society.
4. G.P.Gilfoyle and J.A.Parmentola, ‘Using Nuclear Materials to Prevent Nuclear Proliferation’, *Science and Global Security* **9**, 81 (2001).
5. ‘E5 Status Report’, Plenary Session of the CLAS Collaboration Meeting, October 19, 2002.

Collaborators (2000-2004)

I have worked with many members of the CLAS Collaboration during the last four years. A listing of the full collaboration is available at the following website.

<http://www.jlab.org/Hall-B/general/phonebook.html>

The list below includes members of the Collaboration that I have worked closely with and others outside the Collaboration.

Mac Mestayer	William Brooks	Bernhard Mecking
Lawrence Weinstein	Michael Vineyard	Andrei Afanasev
Philip Cole	Sebastian Kuhn	David Jenkins
Jeffrey Lachniet	Brian Quin	Latifa Elouadrhiri
Kim Egiyan	Rustam Niyazov	Raphaella DeVita
Derek Branford	Harut Avakian	Sabine Jeschonnek
J.W. Van Orden	John Parmentola	Anthony Fainberg
Mark Ito	Eliot Wolin	Arne Freyberger
Ivan Oelrich	Eric Gerdes	Philip Rubin

Special Considerations

None.

Estimate of Unobligated Funds

Approximately \$5,000 will remain at the end of the current project period which is less than 10% of the funding for the current budget period.

Facilities and Resources

Four major components of the University support for the proposed research are: computers, laboratory facilities, travel, and linux support. The computing facilities in the Department of Physics include a 53-node Linux cluster and numerous Linux workstations supported by about five TByte of storage space, tape drives, CD burners, *etc.* The cluster is in a dedicated, 600 – m² laboratory that was renovated for that purpose. All of the workstations in the Department and the cluster are part of a high-speed, campus-wide network.

The Dean of the Faculty of Arts and Sciences agrees to fund travel in the form of mileage to and from Jefferson Lab and occasional overnight lodging and meals associated with research. The Dean's office has also supported travel to other laboratories for research and consultation, and will continue this policy. No fixed dollar allocation has been made for travel, but over the past fifteen years no documented request has been denied.

Two years ago, the University hired its first linux support person. This person has been a valuable asset for improving security, updating software, and upgrading the system.

Current and Pending Support

Source	Title	Amount	Period	Comments
DOE	Nuclear and Particle Physics Research at the University of Richmond	\$218,107	2005-2008	Current Contract Faculty: Gilfoyle

Budget Explanation

First Year: June 1, 2005 - May 31, 2006

A.	Senior Personnel Totals (two-ninths of academic year salary for one faculty member)	
	1. G.P.Gilfoyle	\$17,560
	Total Senior Personnel	\$17,560
B.	Other Personnel Totals (two undergraduate students for ten summer weeks)	
	1. (1) Postdoctoral Associate	\$0
	2. (0) Other Professionals	\$0
	3. (0) Graduate Students	\$0
	4. (2) Undergraduate Students	\$10,000
	Total Other Personnel	\$10,000
	Total Salaries	\$27,560
C.	Fringe Benefit Totals (8.5% for faculty and students)	\$2,343
	Total Salaries, Wages, and Fringe Benefits	\$29,903
D.	Permanent Equipment List (Anticipated cost of six dual-CPU computing nodes to replace aging machines in the existing cluster. See quote in Appendix A and Section 3.3 of the Task Description.)	\$17,280
	Total Permanent Equipment	\$17,280
E.	Travel	
	1. Domestic (travel, lodging, and subsistence for faculty and students to Jefferson Lab and APS meetings)	\$2,500
F.	Trainee/Participant Costs	\$0
G.	Other Direct Costs	
	1. Materials	\$1,000
	2. Page Charges	\$1,000
	3. Consultant Services	\$0
	4. Computer Services	\$0
	Total Other Direct	\$2,000
H.	Total Direct	\$51,683
I.	Total Indirect Costs (52% of salaries, wages, and fringe benefits)	\$15,549
J.	Total Direct and Indirect Costs	\$67,232
K.	Applicant's Cost Sharing	\$0
L.	Final Total	\$67,232

Second Year: June 1, 2006 - May 31, 2007

A.	Senior Personnel Totals (two-ninths of academic year salary for one faculty member)	
1.	G.P.Gilfoyle	\$17,560
	Total Senior Personnel	\$17,560
B.	Other Personnel Totals (two undergraduate students for ten summer weeks)	
1.	(0) Postdoctoral Associate	\$0
2.	(0) Other Professionals	\$0
3.	(0) Graduate Students	\$0
4.	(2) Undergraduate Students	\$10,250
	Total Other Personnel	\$10,250
	Total Salaries	\$27,810
C.	Fringe Benefit Totals (8.5% for faculty and students)	\$2,364
	Total Salaries, Wages, and Fringe Benefits	\$30,174
D.	Permanent Equipment List (Anticipated cost of six dual-CPU computing nodes to replace aging machines in the existing cluster. See quote in Appendix A and Section 3.3 of the Task Description.)	\$17,280
	Total Permanent Equipment	\$17,280
E.	Travel	
1.	Domestic (travel, lodging, and subsistence for faculty and students to Jefferson Lab and APS meetings)	\$2,500
F.	Trainee/Participant Costs	\$0
G.	Other Direct Costs	
1.	Materials	\$1,000
2.	Page Charges	\$1,000
3.	Consultant Services	\$0
4.	Computer Services	\$0
	Total Other Direct	\$2,000
H.	Total Direct	\$51,954
I.	Total Indirect Costs (52% of salaries, wages, and fringe benefits)	\$15,690
J.	Total Direct and Indirect Costs	\$67,644
K.	Applicant's Cost Sharing	\$0
L.	Final Total	\$67,644

Third Year: June 1, 2007 - May 31, 2008

A.	Senior Personnel Totals (two-ninths of academic year salary for one faculty member)	
1.	G.P.Gilfoyle	\$17,560
	Total Senior Personnel	\$17,560
B.	Other Personnel Totals (two undergraduate students for ten summer weeks)	
1.	(0) Postdoctoral Associate	\$0
2.	(0) Other Professionals	\$0
3.	(0) Graduate Students	\$0
4.	(2) Undergraduate Students	\$10,500
	Total Other Personnel	\$10,500
	Total Salaries	\$28,060
C.	Fringe Benefit Totals (8.5% for faculty and students)	\$2,385
	Total Salaries, Wages, and Fringe Benefits	\$30,445
D.	Permanent Equipment List (Anticipated cost of six dual-CPU computing nodes to replace aging machines in the existing cluster. See quote in Appendix A and Section 3.3 of the Task Description.)	\$17,280
	Total Permanent Equipment	\$17,280
E.	Travel	
1.	Domestic (travel, lodging, and subsistence for faculty and students to Jefferson Lab and APS meetings)	\$2,500
F.	Trainee/Participant Costs	\$0
G.	Other Direct Costs	
1.	Materials	\$1,000
2.	Page Charges	\$1,000
3.	Consultant Services	\$0
4.	Computer Services	\$0
	Total Other Direct	\$2,000
H.	Total Direct	\$52,225
I.	Total Indirect Costs (52% of salaries, wages, and fringe benefits)	\$15,831
J.	Total Direct and Indirect Costs	\$68,057
K.	Applicant's Cost Sharing	\$0
L.	Final Total	\$68,057

Appendix

A Compute Node Quote

i2X
Optimized. Scalable.
clusterBlocks™

533series™ | procNode
Simplifying cluster procurement, deployment, and management.
Certified Nimitz

i2X procNode Features Matrix Configurations : 1U i2XPZA.1 > i2XPZA.6

i2XPZA procNode Baseline Configuration Description :
 1U Rackmount chassis / (1) 40GB / 2GB ECCR-DDR / (2) 1000e onboard / Rails
 LinuxBIOS, Nimbus Cluster OS distribution (latest commercial version), HotSwap Nodes, Bproc/SSI support, Driver optimizations

i2XPZA procNode Baseline Component Itemization :

	Manuf	Qty
1U Rack Mount Chassis Plain front bezel 420w UL x 1	Supermicro®	30
Supermicro® 7501/533 X5DPI-G2 Dual Xeon xATX motherboard	Supermicro®	30
Intel® P4 Xeon® XXXGHz 533FSB s603 PGA 512k	Intel®	60
1U Xeon CPU Cooler	OEM	60
1U Xeon CPU Cooler retention module	OEM	60
4GB Config (512MB x8) 2.5v 184-pin DDR-266 PC-2100 ECC Registered Low-Profile for 1U (2.4 DIMM sockets)	CMTL® certified	240
Seagate® 40GB EIDE S/ATA-100 7200rpm 3.5" internal HDD (internal)	Seagate®	30
64-bit 1U PCI-X Riser 3.3/5v universal for installed controller	Supermicro®	30
Solid-baring slide-rail kit for 1U chassis	OEM	30
M6 x 16 Screws Stainless Steel / Zinc coated , Phi/Slot heads	hpcNetwork®	300
M6 Cage Nuts (3307) Stainless Steel / Zinc coated	hpcNetwork®	300
Assemble and Testing [SCC]	SourceCode®	30
Pre-racking, pre-wiring fee per node	SourceCode®	30
Wiring and Rack decals and stickering	SourceCode®	30

i2XPZA procNode Options Index :

	Manuf	Qty
Default Onboard: 1000e Ethernet Port(s)	Intel®	60

i2X procNode Environmental Data Configurations : 1U i2XPZA.1 > i2XPZA.6

i2XPZA Environmental Data Methodology :
 Calculations for thermal (BTU/hr) outputs and power (Watts) consumption are general and conservative.
 1U Testing = 350/420w UL PS, (2) Xeon 2.8GHz, (8) 1GB DDR, (2) 73GB SCSI, CD, FDD, PCI-X 5v
 All clusterBlocks™ systems are stress-tested to insure reliable high-density/availability usage.

i2XPZA procNode Racking Allocations (1.75" vertical U requirement) :

i2X series	Unit 1.75" U	Allocated 1.75" U	25,00
	1		

i2XPZA procNode Thermal Calculations (BTU/hr) :

i2XPZA.1 > .6	Unit BTU/hr	Total BTU/hr	45000.7
	1554.51		

i2XPZA headNode Power Consumption Calculations (Watts) :

i2XPZA.1 > .6	Unit Watts	Total Watts	13139.23
	453.08		

i2X procNode Pricing Schedules Configurations : 1U i2XPZA.1 > i2XPZA.6

i2XPZA procNode Full Configuration Description / Pricing :

procNode Configuration	Unit		USDs
	Manuf BOM	Model	
Dual Intel® Xeon® 2.40GHz 533FSB s603 PGA 0512k	Next	i2XPZA.1	\$2,617.80
Dual Intel® Xeon® 2.66GHz 533FSB s603 PGA 0512k	Next	i2XPZA.2	\$2,649.00
Dual Intel® Xeon® 2.80GHz 533FSB s603 PGA 0512k	Next	i2XPZA.3	\$2,754.60
Dual Intel® Xeon® 3.06GHz 533FSB s603 PGA 0512k	Next	i2XPZA.4	\$2,879.40
Dual Intel® Xeon® 3.06GHz 533FSB s603 PGA 1024k	Next	i2XPZA.5	\$3,203.11
Dual Intel® Xeon® 3.20GHz 533FSB s603 PGA 1024k	Next	i2XPZA.6	\$3,731.11

procNode Configuration	Aggregate		USDs
	Manuf BOM	Model	
Dual Intel® Xeon® 2.40GHz 533FSB s603 PGA 0512k	Next	i2XPZA.1	\$79,534.00
Dual Intel® Xeon® 2.66GHz 533FSB s603 PGA 0512k	Next	i2XPZA.2	\$79,470.00
Dual Intel® Xeon® 2.80GHz 533FSB s603 PGA 0512k	Next	i2XPZA.3	\$82,638.00
Dual Intel® Xeon® 3.06GHz 533FSB s603 PGA 0512k	Next	i2XPZA.4	\$86,382.00
Dual Intel® Xeon® 3.06GHz 533FSB s603 PGA 1024k	Next	i2XPZA.5	\$96,084.00
Dual Intel® Xeon® 3.20GHz 533FSB s603 PGA 1024k	Next	i2XPZA.6	\$111,924.00

B Richmond Computing Cluster Users and Projects

This section contains descriptions of three major projects by outside users that are done on the Richmond computing cluster. Individual accounts are given to the users and limited support is provided by me and the Linux support technician on the University's information services staff [31].

B.1 Pion Photoproduction with CLAS (*D.Jenkins, Virginia Tech*)

The University of Richmond cluster has been very useful during the past year as a means for studying the acceptance of Jefferson Lab's CLAS detector. Although Jefferson Lab has a large computer farm, it's priority for data reduction allows little time for Monte Carlo calculations. There are several projects that could be done over the next few years if time continues to be available on the Richmond cluster. These include additional studies of acceptances, the calculation of acceptances for data analysis of pion-photoproduction experiments, a study of the feasibility of adding new counters to the CLAS scintillation array at forward angles, planning for future measurements of spin observables in meson photoproduction, and the data reduction of these measurements. All of the work has the goal of contributing to a better understanding of the excited states of baryons.

Results from calculations on the cluster were used in a recently completed work that considered the affect of pion decay upon the pion's acceptance, CLAS Note 2004-35. Current calculations are looking at the influence of scattering that could change the particle's reconstructed angle giving the wrong angular distribution for the detected particle. The influence upon acceptance is found by comparing the simple acceptance that ignores scattering processes, and the full acceptance that includes them. Other acceptance studies will seek to make corrections for the difference in yields in the six sectors of the detector. Understanding the differences is important for a determination of systematic errors.

Once the acceptances are understood and means are found for determining their errors, work can proceed with the analysis of data from experiment E-94-103, The Photoproduction of Pions from Protons and Neutrons. The goal of the analysis is to measure the differential-cross-sections with accuracy better than 3%. The evaluation of the cross section will require extensive calculations of the acceptance to get good statistics for the full energy and angular range observed in the experiment. To accumulate data in bin widths of 20 MeV in photon energy and 5 degrees in angle with 6 sectors, about 20,000 bins will be needed. A statistical error of 0.5% for the acceptance in each bin will require an average of 40,000 counts per bin, or a total of about 8×10^8 events in the simulation for each reaction channel

While data from past experiments is analyzed, new experiments are being prepared to look at spin observables. To get maximum information from these experiments, the data must be collected over as wide an angular range as possible so that uncertainties can be reduced in subsequent partial-wave analyses. Measurements at forward angles can be important for those reactions in which the observables have a large value at small angle. The feasibility of adding a new counter at forward angles for each sector of the scintillation-counter array will be considered. The study will require computer simulations to investigate the improvement obtained by such a counter.

The new measurements of spin observables will look at photoproduction of pions, etas and kaons with polarized beams and targets. The experiments that will make use of the Richmond cluster are include E-02-112, Search for Missing Nucleon Resonances in the Photoproduction of Hyperons Using A Polarized Photon Beam and A Polarized Target; E-03-105, Pion Photoproduction from a Polarized Target; E-04-102, Helicity Structure of Pion Photoproduction; and a new experiment, to be submitted, that will observe spin observables for eta photoproduction. The purpose of these experiments is to improve the extraction of reaction parameters from partial-wave analyses and thus give a better determination of the spectra of baryon resonances. The experiments will require extensive computer simulations for their planning and data reduction.

B.2 Radiative Corrections for E94-017 (*J.Lachniet, B.P.Quin, CMU*)

Nucleon structure is one of the most fundamental issues in nuclear physics. Elastic electron scattering provides detailed information about the electromagnetic structure of the nucleon. The differential cross section for elastic electron-nucleon scattering in the one-photon-exchange approximation is given by the Rosenbluth formula in which the nucleon structure information is contained in the Sachs electric and magnetic form factors. These form factors are used for comparison between experiment and theoretical models of nucleon structure. In addition to being of fundamental importance in understanding nucleon structure, the form factors are a necessary input for calculations of nuclear response functions. Although the proton form factors are well determined, the present knowledge of the neutron form factors is inadequate to impose severe constraints on nucleon structure models. Reliable separations of the two form factors have been made up to $Q^2 = 9(\text{GeV}/c)^2$ for the proton, but only to $Q^2 = 4(\text{GeV}/c)^2$ for the neutron. Also, the neutron form factors have been determined with much less precision than those of the proton. The reason for the large uncertainties in the neutron measurements is that most of these data come from analyses of inclusive quasielastic electron scattering from deuterium that introduce a number of significant systematic errors. In this experiment, precise measurements of the ratio of quasielastic electron-neutron to electron-proton scattering in deuterium were made over a Q^2 range from 0.3 to 7.5 $(\text{GeV}/c)^2$ with the CLAS. The neutron magnetic form factor will be extracted from this ratio with the use of the more accurately known proton form factors. Data was taken simultaneously on separated hydrogen and deuterium targets. The $e + p \rightarrow e + n + \pi^+$ reaction on the hydrogen target has been used to measure the neutron detection efficiency. The data from electron-proton and electron-neutron scattering in deuterium will be treated in an identical way insofar as possible. The use of this ratio technique, with the simultaneous calibration of the neutron detection efficiency, significantly reduces or eliminates many of the systematic errors associated with quasielastic scattering from deuterium.

The measured neutron form factors typically have to be corrected for radiative effects. The expectation is these effects would cancel completely or at least be minimized by using the ratio method described above. However, these measurements are exclusive ones and most treatments of radiative corrections do not account for this exclusivity. As a result the program EXCLURAD originally developed for the exclusive $p(e, e'\pi^+)n$ reaction has been modified for $d(e, e'p)n$. See Section 2.2.1 for more details. This modified version requires considerable computer time so the calculations will be run on the Richmond cluster. The initial results show the effect of radiative corrections on the neutron form factor measurement are small using the ratio method (see Section 2.2.1). Many more cases have to run before the project is complete.

B.3 Analysis of Exclusive η Photoproduction in Nuclei (*M.F. Vineyard, Union College*)

Through the study of the excitation, propagation, and decay of nucleon resonances in the nuclear environment one expects to understand eventually how the strong interaction is affected by baryon structure. A wealth of information on the $\Delta(1232)$ and its dynamics within the nuclear medium has been obtained through pion studies. However, very little is known about medium properties of the higher energy excited states of the nucleon. This is primarily due to the fact that the dominance of the Δ and the overlapping of high resonances prevents studying one specific state by π -production experiments. The η meson, on the other hand, couples only with isospin 1/2* resonances since it is an isoscalar particle, and therefore provides an excellent way to isolate these resonances. In this experiment, inclusive measurements of the photoproduction of η mesons in nuclei were made

to investigate medium modifications of the $S_{11}(1535)$ and $P_{11}(1710)$ resonances which are the only nucleon resonances of mass less than 2 GeV with significant η decay branches.

These measurements will also provide information on the η decay branches. Due to the lack of η beams, very little is known about the interaction of η mesons with nucleons. In this equipment, final-state interactions of the η meson propagating through the nucleus is being used to investigate the ηN interaction. The study of η interactions with nucleons and nuclei can provide significant tests of our understanding of meson interactions which has been developed through pion studies. Also, a comparative study of the response of η and η' mesons in the nuclear environment may provide insight into the mixing in these two mesons and the structure of the η' .

The experiment was performed with the CEBAF Large Acceptance Spectrometer (CLAS) and bremsstrahlung tagging system in Hall B. Tagged photons with energies between 0.8 and 1.5 GeV were incident on ^2H , ^4He , and ^{12}C targets. The η mesons were detected with the CLAS via the two-photon decay. The first-pass analysis ('cooking') is complete and the data have been transported to the Richmond cluster. The cluster will be used for second-pass analysis and simulation of the CLAS response.

Out-of-Plane Measurements of the Structure Functions of the Deuteron

G.P.Gilfoyle

Physics Department, University of Richmond, VA, 23173 USA

W.K.Brooks, B.A.Mecking

*Thomas Jefferson National Accelerator Facility, 12000 Jefferson Avenue,
Newport News, VA 23606, USA*

S.Kuhn, L.Weinstein

Physics Department, Old Dominion University, Norfolk, VA, 23529, USA

M.F.Vineyard

Physics Department, Union College, Schenectady, New York, 12308 USA

Abstract

We propose the measurement of the structure functions of the deuteron f'_{LT} , f_{TT} , and f_{LT} using the reaction $d(\vec{e}, e'p)n$ with CLAS. The 'standard model' of nuclear physics is not well-developed in the GeV region, and the relative importance of relativistic corrections, final-state interactions, meson-exchange currents, and isobar configurations is unknown. These data will provide a baseline for conventional nuclear physics, so deviations from the model at higher Q^2 can be attributed to quark-gluon effects with greater confidence. The three structure functions will be extracted by measuring different moments of the out-of-plane production in CLAS. Each of these moments is related to a different asymmetry which is, in turn, proportional to a particular structure function. The structure function f'_{LT} is nonzero only in the out-of-plane production. This analysis will be performed on the existing E5 data set that covers the range $Q^2 = 0.2 - 5.0$ (GeV/c)². We will study the reaction in quasi-elastic kinematics first and later investigate higher energy transfers. Our preliminary results show we can observe small asymmetries with good precision in quasi-elastic kinematics.

Approved by the CLAS Collaboration, November 14, 2003.

1 Introduction

We propose to analyze existing CLAS data from the E5 running period to extract the structure functions f_{LT} , f_{TT} , and f'_{LT} of the deuteron using the proton azimuthal distribution from the $d(\vec{e}, e'p)n$ reaction. Electron scattering from the deuteron is an essential testing ground for any model of the nucleon-nucleon force. It is the simplest nucleus in nature and the electromagnetic interaction is well-known and weak (so it can be treated in first-order perturbation theory). The structure functions describing the electromagnetic response of nuclei are sensitive to a variety of phenomena depending on the choice of kinematics, *i.e.* the energy transfer ν and the 4-momentum transfer Q^2 . Using a polarized beam and the large acceptance of the CLAS detector we will break new ground in the investigation of the structure function f'_{LT} which is non-zero only for the out-of-plane production. This analysis will focus on the quasi-elastic regime first to study the Q^2 evolution of the structure functions from the better-known, low- Q^2 region where data now exist up to the GeV region where there are few measurements and our theoretical understanding is incomplete. The quasi-elastic structure functions are also less sensitive to some of the non-nucleonic degrees-of-freedom so they serve as a benchmark for other kinematic regions. We will later push this study beyond the quasi-elastic region to higher energy transfers.

Understanding the deuteron tests the ‘standard’ or hadronic model of nuclear physics. The goal is to construct a ‘consistent and exact description’ of few-body nuclei (^2H , ^3H , ^3He , ^4He) [1]. For example, it is an open question whether a single interaction or current operator can account for the attributes of all these nuclei. Calculations using hadronic effects like meson-exchange currents (MEC), isobar configurations (IC), and final-state interactions (FSI) are under development, but have yet to be fully challenged by data in the GeV region [1, 2]. The influence of relativity is also being studied [1, 2, 3, 4, 5]. Previous results at lower Q^2 reveal the onset of many of these effects so a complete, modern calculation is needed to compare with data across the full range of Q^2 to test and understand the hadronic model in this region. It is worth mentioning these issues were raised as ‘Key Questions’ at the Jefferson Laboratory PAC14 Few-Body Workshop [1].

Of equal importance is finding where and how the ‘standard model’ of nuclear physics breaks down; requiring quark-gluon or quark and flux-tube degrees-of-freedom. Studying this transition is an essential goal of nuclear physics [1, 7]. The basic idea is that if we cannot describe observations with all of the pieces mentioned above, then we would see genuine quark effects in the nucleus. Clearly, we cannot make that leap without getting firm control of the calculations using the hadronic degrees-of-freedom. It is expected that transition will occur in the GeV region [2, 7].

Out-of-plane measurements probe components of the electromagnetic response of the deuteron that are difficult or impossible to investigate otherwise. The deuteron’s electromagnetic structure is studied via electron scattering which is characterized by a set of response functions that connect model calculations and measurements. Typically, (*i.e.*, with unpolarized targets and detectors that all lie in the scattering plane), there are four response functions determined by different combinations of the longitudinal and transverse components of the electromagnetic current. However, with polarized electron beams and measurements of the ejected proton out of the scattering plane of the electron, a new response function can be measured. This fifth response function f'_{LT} is the imaginary part of the interference between the longitudinal and transverse parts of the electromagnetic current. The same experimental capabilities can also separate the longitudinal-transverse response function f_{LT} and the transverse-transverse response function f_{TT} [8]. The influence of different phenomena (*e.g.*, relativity, FSI, *etc.*) varies with the each of the structure functions and depends on the choice of kinematics. For example, f'_{LT} is more sensitive to relativistic corrections than f_{TT} , but this sensitivity declines in the dip region. Measuring the out-of-plane behavior is a tool for unraveling the deuteron’s electromagnetic response. Progress in making these sorts of measurements has required rather substantial efforts and, as a consequence, produced limited data sets. The CLAS detector is inherently an out-of-plane detector and is ideally suited for studying the out-of-plane behavior of the electromagnetic structure functions of the deuteron.

We propose here to analyze already-collected data of the $d(\vec{e}, e'p)n$ reaction from the CLAS E5 running period. About 2.3 billion triggers were collected during this run period in the range $Q^2 = 0.2 - 5.0$ (GeV/c) 2 using a dual-cell target containing deuterium (as the primary target) and hydrogen (for *in situ* calibrations). Three sets of run conditions were used: 4.23 GeV with a normal torus field polarity, 2.56 GeV with a normal torus field polarity, and 2.56 GeV with a reversed torus field polarity to reach lower Q^2 . Cooking of the data was completed in late 2002. We will extract three structure functions f_{LT} , f_{TT} , and f'_{LT} by studying the

variation of the cross section on ϕ_{pq} , the angle between the scattering plane of the incoming and scattered electron and the reaction plane of the ejected proton and neutron. The kinematic range of the measurements will enable us to study the Q^2 evolution from the upper limit of most previous studies of these structure functions ($Q^2 \approx 0.2$ (GeV/c)²) to a region where some models are expected to fail (at $Q^2 \approx 1.0$ (GeV/c)²). These measurements will be compared with several different theoretical calculations.

Below, we develop the formalism used to analyze the electromagnetic response functions and discuss the current status of experiment and theory. We then show how CLAS will be used to make out-of-plane measurements and demonstrate the feasibility of those measurements. We then summarize our results.

2 Formalism for $d(e, e'p)X$

For the case of a polarized electron beam incident on an unpolarized target, the three-fold differential cross section can be written in the one-photon exchange approximation as

$$\begin{aligned} \frac{d^3\sigma}{d\nu d\Omega_e d\Omega_p} = & c\{\rho_L f_L + \rho_T f_T + \rho_{LT} f_{LT} \cos(\phi_{pq}) \\ & + \rho_{TT} f_{TT} \cos(2\phi_{pq}) + h\rho'_{LT} f'_{LT} \sin(\phi_{pq})\} \end{aligned} \quad (1)$$

where

$$c = \frac{\alpha E'}{6\pi^2 Q^4 E} \quad , \quad (2)$$

α is the fine-structure constant, E and E' are the incoming and outgoing electron energies respectively, Q^2 is the square of the 4-momentum transfer, h is the electron beam helicity (± 1), the $\rho_{\lambda\lambda'}$ are the virtual-photon density matrix elements which depend only on the electron kinematics (see Reference [9]), and the $f_{\lambda\lambda'}$ are the response functions in the center of mass. The azimuthal angle ϕ_{pq} is the angle between the scattering plane defined by the incoming and outgoing electrons and the reaction plane defined by the ejected proton and neutron (see figure below). The response functions depend on the energy transfer ν , the 3-momentum

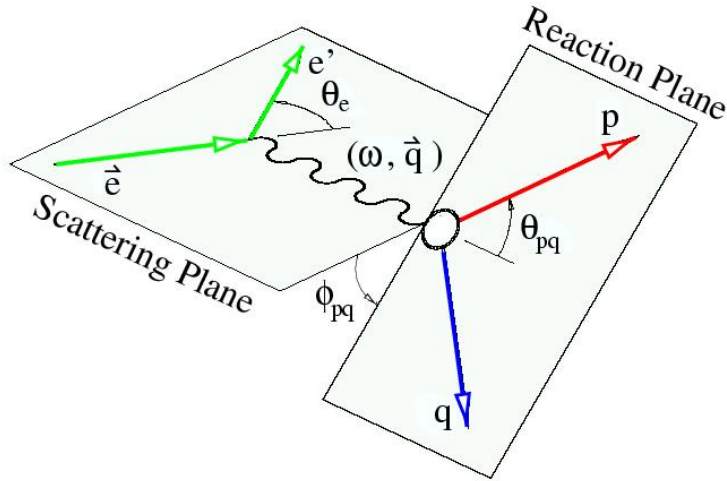


Figure 1: Kinematic quantities for $d(\vec{e}, e'p)n$.

transfer \vec{q} , and θ_{pq}^{cm} where θ_{pq}^{cm} is the angle between \vec{q} and the ejected proton momentum in the center-of-mass frame. The missing momentum is often used to describe this reaction and is

$$\vec{p}_m = \vec{q} - \vec{p}_p \quad (3)$$

where \vec{p}_p is the ejected proton momentum. In the plane-wave impulse approximation this missing momentum is the opposite of the initial momentum of the proton.

When using conventional, small-acceptance, spectrometers, one approaches the problem of extracting the response functions by constructing asymmetries to isolate different components. Consider the following asymmetries measured at azimuthal angle ϕ_{pq} around the \vec{q} vector.

$$A_{LT} = \frac{\sigma_{0^\circ} - \sigma_{180^\circ}}{\sigma_{0^\circ} + \sigma_{180^\circ}} = \frac{\rho_{LT} f_{LT}}{\rho_L f_L + \rho_T f_T + \rho_{TT} f_{TT}} \quad (4)$$

$$A'_{LT} = \frac{\sigma_{90^\circ}^{(+1)} - \sigma_{90^\circ}^{(-1)}}{\sigma_{90^\circ}^{(+1)} + \sigma_{90^\circ}^{(-1)}} = \frac{\rho' f'_{LT}}{\rho_L f_L + \rho_T f_T - \rho_{TT} f_{TT}} \quad (5)$$

$$A_{TT} = \frac{\sigma_{0^\circ} + \sigma_{180^\circ} - 2\sigma_{90^\circ}}{\sigma_{0^\circ} + \sigma_{180^\circ} + 2\sigma_{90^\circ}} = \frac{\rho_{TT} f_{TT}}{\rho_L f_L + \rho_T f_T} \quad (6)$$

The subscripts refer to the value of ϕ_{pq} and the superscripts refer to the beam helicity. Note that in each case one divides by the sum of the measurements so that systematic uncertainties will be reduced. Each asymmetry is proportional to one of the response functions in Equation 1 so one can investigate the behavior of these terms in the cross section. One can combine Equations 4–6 and rearrange to get expressions for f_{LT} , f_{TT} , and f'_{LT} .

$$f_{LT} = \frac{\sigma_{0^\circ} - \sigma_{180^\circ}}{2c\rho_{LT}} \quad (7)$$

$$f'_{LT} = \frac{\sigma_{90^\circ}^{(+1)} - \sigma_{90^\circ}^{(-1)}}{2c\rho'_{LT}} \quad (8)$$

$$f_{TT} = \frac{\sigma_{0^\circ} + \sigma_{180^\circ} - 2\sigma_{90^\circ}}{4c\rho_{TT}} \quad (9)$$

These results (Equations 7–9) show how these response functions are determined from out-of-plane measurements with conventional spectrometers. Below we will discuss how to take advantage of the large acceptance of CLAS in making similar measurements.

3 Current Status

In this section we describe the world data for each of the three structure functions f'_{LT} , f_{TT} , and f_{LT} . We then show the relationship of this proposal to other Jefferson Lab experiments.

The measurements for f'_{LT} are sparse, but have given us a glimpse of the the physics to come. They require out-of-plane spectrometers and polarized beams. For quasi-elastic kinematics they have only been made at $Q^2 = 0.22$ (GeV/c)² and $Q^2 = 0.13$ (GeV/c)² at Bates [8, 10, 11]. The results are shown in Figure 2. That work demonstrated the utility of out-of-plane measurements and the calculations presented show that relativity already plays a significant role even at this low value of Q^2 [5]. In the right-hand panel of Figure 2, the solid curve includes relativistic corrections and is noticeably different from the other curves. The effect of final-state interactions is dramatic and can be seen in the left-hand panel of Figure 2. The double-dot-dashed line at $f'_{LT} = 0$ is from a Plane-Wave Born Approximation calculation which does not include FSI. In general, f'_{LT} is non-zero only in the presence of final-state interactions. The other calculations do include FSI and they are all significantly different from zero. Unfortunately, the large uncertainties of the data prevent one from distinguishing among different effects like MEC, FSI, and IC or between different potentials. The calculations in Reference [10] (left-hand panel of Figure 2) by Arenhövel at $Q^2 = 0.13$ (GeV/c)² employed four different potentials and include effects from MEC, Δ -isobar contributions (IC), and relativistic corrections (RC). The calculations were insensitive to MEC and IC, but relativistic corrections make a noticeable contribution; about the same effect as the difference between different potentials. The calculations at $Q^2 = 0.22$ (GeV/c)² (right-hand panel of Figure 2) display a similar behavior. These studies have revealed the importance of relativity and FSI in this region of Q^2 . The success of the Bates work at low Q^2 is an invitation to extend the measurements with CLAS. CLAS is an out-of-plane detector by its very nature so the analysis of the E5 data will dramatically improve the state-of-the-art of these measurements.

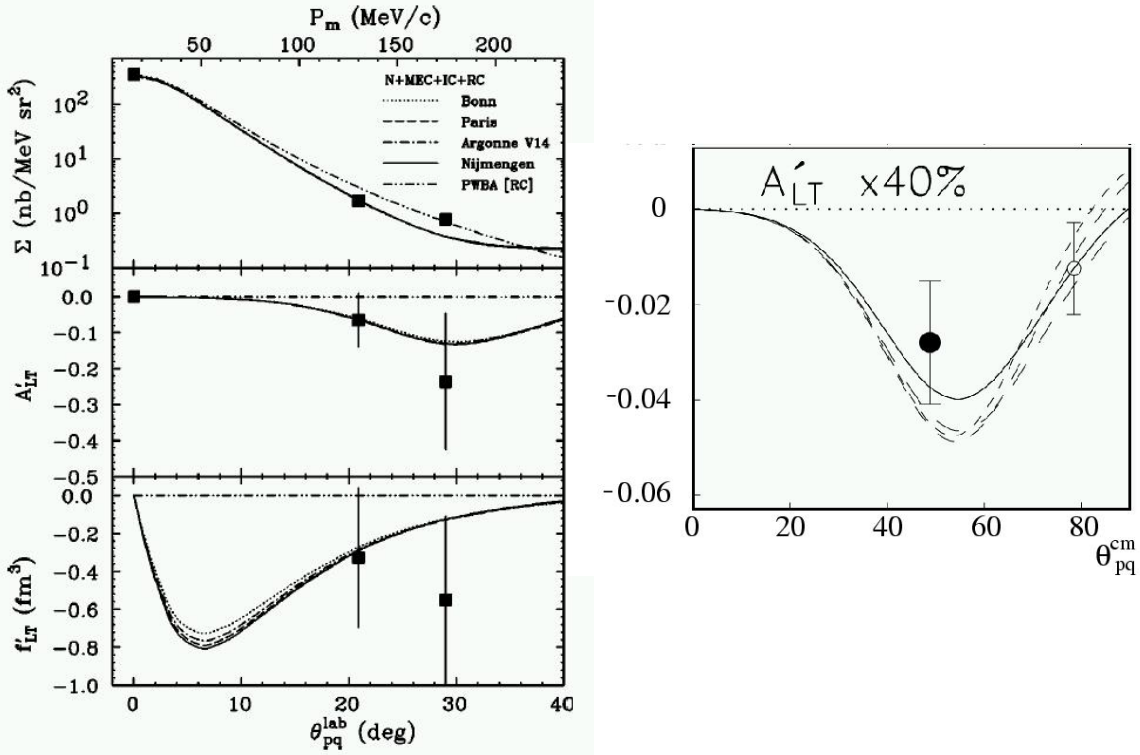


Figure 2: Measurements of f'_{LT} and its associated cross section and asymmetry from Reference [10] at $Q^2 = 0.13 \text{ (GeV/c)}^2$ (left-hand panel) and A'_{LT} from Reference [8] at $Q^2 = 0.22 \text{ (GeV/c)}^2$ (right-hand panel). The observations in the left-hand panel are shown as a function of θ_{pq}^{lab} in degrees and the ones in the right-hand panel are shown as a function of θ_{pq}^{cm} in degrees. The open circle is for anticipated data.

The situation is little different for observations of the transverse-transverse interference term f_{TT} in quasi-elastic kinematics. These experiments require out-of-plane measurements and unpolarized beam, but this portion of the cross section must be separated from the larger contributions of f_L , f_T , and f_{LT} . Three measurements have been made at Tohoku ($Q^2 = 0.013 \text{ (GeV/c)}^2$), NIKHEF ($Q^2 = 0.21 \text{ (GeV/c)}^2$), and Bates ($Q^2 = 0.22 \text{ (GeV/c)}^2$) [8, 12, 13]. The lowest Q^2 measurements agree with a non-relativistic calculation which uses the Paris potential and includes the effect of MEC and IC, but the data have large uncertainties. The NIKHEF experiment could only put an upper limit on the structure function because it was combined with the larger longitudinal structure function f_L . The Bates results have smaller uncertainties than in the f'_{LT} case (see Figure 3 and compare with Figure 2), but one still cannot distinguish among MEC, FSI, RC, and IC effects. There is a clear need here to reduce the uncertainties and extend the measurements out to larger θ_{pq}^{cm} where the calculations diverge. Again, because of the considerable out-of-plane capabilities of CLAS we expect to significantly improve the state-of-the-art of these measurements.

The longitudinal-transverse interference structure function f_{LT} has been measured several times and with greater precision than the other two structure functions above. At the lowest $Q^2 = 0.013 \text{ (GeV/c)}^2$ the data are reproduced by a non-relativistic calculation while at the highest ($Q^2 = 1.2 \text{ (GeV/c)}^2$) the relativistic calculations of the asymmetry are preferred [12, 14]. Between these two extremes, the situation is less clear. At $Q^2 = 0.15 \text{ (GeV/c)}^2$ data from NIKHEF were compared with calculations by Hummel and Tjon which include RC and FSI and calculations by Arenhövel that are non-relativistic but include MEC, IC, and FSI [13, 15, 16, 17]. The results for the combined f_L and f_{TT} structure function could not discriminate between the two calculations, but the results for f_{LT} favored the relativistic calculation of Hummel and

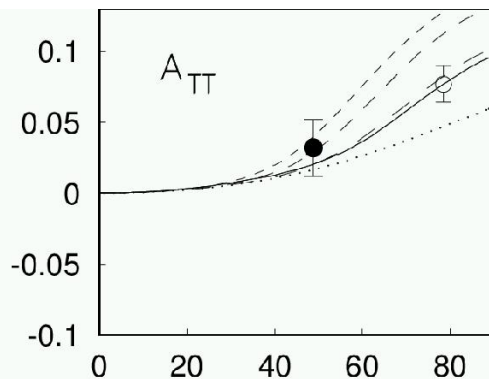


Figure 3: Measurements of f_{TT} as a function of θ_{pq}^{cm} for quasi-elastic kinematics from Reference [8]. The filled circle is the data, the open circle shows expected future results

Tjon. Measurements of f_{LT} at similar Q^2 at Bates and Saclay agree better with non-relativistic calculations by Arenhövel than with the same relativistically corrected ones [18, 19]. The Arenhövel calculations include MEC in the Saclay work and MEC, FSI, and IC in the Bates experiment. In the Saclay work, there is a ‘disconcerting’ spread among the relativistic calculations suggesting the need to improve these calculations by performing experiments at higher Q^2 [19]. A nearby measurement at $Q^2 = 0.145 \text{ (GeV/c)}^2$ clearly favors the inclusion of relativity [20]. It is worth noting that a recent measurement of the cross section in the middle of this region ($Q^2 = 0.67 \text{ (GeV/c)}^2$) was reproduced with a calculation by Arenhövel that includes relativistic effects, FSI, MEC, and IC [21, 22]. The E5 data spans the Q^2 range of the observations discussed here so this analysis project holds the promise of connecting the picture of the deuteron at low Q^2 to high Q^2 . In addition, the E5 data have considerable overlaps and consistency checks among the three sets of run conditions.

As one moves away from the quasi-elastic region the mixture of physics effects changes. The data show an increased sensitivity to MEC and IC effects for f_{TT} in the dip and Δ regions and are not influenced by RC or FSI [8, 23]. The other structure functions f_{LT} and f'_{LT} are the opposite; sensitive to RC and FSI effects and independent of MEC and IC. Unfortunately, the data are sparse and often have large uncertainties.

In summary, several points can be made about our current understanding of the deuteron structure functions. First, different structure functions are influenced by different physics. The f_{LT} and f'_{LT} structure functions are sensitive to relativistic effects and f'_{LT} is especially sensitive to final state interactions. The other structure function in our study, f_{TT} , is more sensitive to non-nucleonic degrees of freedom (MEC and IC). Second, the different kinematic regimes probe different physics. On the quasi-elastic ridge, MEC and IC contribute little, but their effect increases as one moves into the dip and Δ regions while the impact of RC and FSI declines. Finally, there is little data in the range $Q^2 = 0.2 - 1.0 \text{ (GeV/c)}^2$ where it is needed to unravel all of the competing effects mentioned above.

This analysis project will complement other experiments at Jefferson Lab. Experiment E02-101 (K. Wang spokesperson and contact) is designed to extract all the structure functions f_L , f_T , f_{LT} , f_{TT} , and f'_{LT} at threshold for $Q^2 = 0.47 \text{ (GeV/c)}^2$ using the HRS and BigBite spectrometers in Hall A. Threshold kinematics have been chosen to minimize the contribution of nucleonic effects to study the effects of RC, MEC, and IC. Our study of quasi-elastic effects reduces the influence of non-nucleonic degrees of freedom (MEC and IC) so we are exploring different physics. In addition, E02-101 will take data at a single Q^2 while the CLAS data cover a larger kinematic region. Figure 4 displays a comparison of the kinematic coverage of E01-020 and this analysis. The red, green, and blue areas show the kinematic coverage for the three sets of run conditions for the E5 run period. The square is the proposed kinematics for E02-101. The quasi-elastic ridge can be clearly seen along the low- ν edge of the E5 kinematics. There is also a large amount of data at higher ν or W that will be analyzed.

Experiment E01-020 has two parts made up of two previous proposals: PR-01-007 (formerly E94-004, W.Boeglin spokesperson and contact) and PR-01-008 (P.Ulmer spokesperson and contact). Data collection

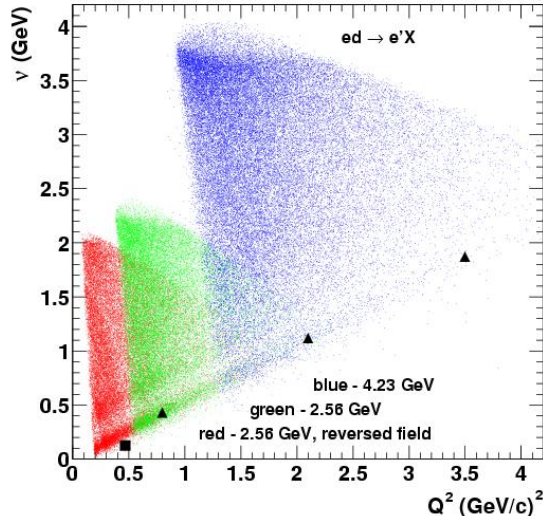


Figure 4: Energy loss of the electron versus Q^2 . The red, green, and blues areas represent the kinematic coverage for the three running conditions during the E5 run period. The triangles are the kinematics for the measurement of σ_{LT} for E01-020. The square is the anticipated kinematics for E02-101.

for this experiment was completed in fall, 2002 in Hall A. In the first part (the former E94-004) parallel and anti-parallel kinematics will be used to study the short-range structure of the deuteron. Perpendicular kinematics at the quasi-elastic peak will be used to extract f_{LT} at $Q^2 = 0.8, 2.1, \text{ and } 3.5 \text{ (GeV/c)}^2$. The measurement of f_{LT} in this experiment overlaps with our proposed analysis project. However, we will be able to extract f_{TT} and f'_{LT} using our out-of-plane measurements. The CLAS detector has lower resolution, but greater kinematic coverage so the two experiments will provide a cross-check for each other. See Figure 4 for a comparison of the kinematics of E01-020 with this analysis.

In the second part of E01-020, the angular distribution of the quasi-elastic peak will be measured at the same values of Q^2 and with recoil momenta between $0.2 \text{ GeV}/c$ and $0.5 \text{ GeV}/c$. The goal is to study FSI and non-nucleonic degrees of freedom (MEC and IC). The measurements will be entirely in the scattering plane. The kinematic region overlaps with the CLAS data of this proposed analysis, but no effort will be made to extract the structure functions.

To summarize, the analysis of the E5 data to extract the structure functions in the range $Q^2 = 0.2 - 5.0 \text{ (GeV/c)}^2$ from the out-of-plane data will explore new territory. The world's data for f'_{LT} and f_{TT} are sparse and few exist in the Q^2 range covered here. There are more measurements of f_{LT} , but the interpretation of the results is inconsistent which may mean that our understanding of the deuteron is incomplete. The new measurements proposed here are in a Q^2 region where the onset of relativistic effects is increasingly important and contradictory results exist from past work. A systematic study of the out-of-plane structure functions across a wide range in Q^2 will shed light on this problem. The precision of the data may also permit the study of other effects like MEC and IC. The analysis will also complement other experiments at Jefferson Lab to study the deuteron.

4 Measuring Response Functions with CLAS

4.1 Introduction

In this section we discuss our preliminary results and show that the proposed analysis project is feasible. We have measured A'_{LT} on a subset of the E5 data and demonstrated that we can extract this small deuteron structure function with adequate precision to evaluate the success of different theoretical models. The

analysis here is restricted to the quasi-elastic peak so we can compare our results to previous measurements at Bates at lower Q^2 . The theoretical description of the deuteron structure functions is simpler for quasi-elastic kinematics because contributions from meson-exchange currents (MEC) and isobar configurations (IC) are expected to be smaller [10]. In this section we will discuss data selection and corrections, extracting A'_{LT} with different methods, and present some preliminary results.

4.2 Data Selection and Corrections

We are investigating the $d(\vec{e}, e'p)n$ reaction by detecting the scattered electron and the ejected proton with CLAS and using missing mass to identify the neutron. The data were collected during the E5 run period (Spring, 2000) and consist of runs 24020–24588. About 2.3 billion triggers were collected under three sets of run conditions: (1) $E_{beam} = 4.23$ GeV, $I_{torus} = 3375$ A, normal polarity (inbending electrons), (2) $E_{beam} = 2.56$ GeV, $I_{torus} = 2250$ A, normal polarity, and (3) $E_{beam} = 2.56$ GeV, $I_{torus} = 2250$ A, reversed polarity (outbending electrons) to reach lower Q^2 . Electrons were identified as negative tracks from the EVNT bank (produced by SEB) in coincidence with hits in the Cerenkov counters, the TOF scintillators, and the electromagnetic calorimeter. A cut on the number of photo-electrons of greater than 2.5 from the Cerenkov counters was imposed to reduce the number of negative pions misidentified as electrons [24]. Protons were taken from the EVNT bank. Figure 4 above shows the two-dimensional distribution of the energy loss of the electron versus Q^2 . The large kinematic coverage can be seen as well as the extensive overlaps between the different data sets. These overlaps will provide cross checks on the analysis. The acceptance of CLAS for ep coincidences is, on average, 20-30%. Figure 5 shows the missing mass versus θ_{pq}^{cm} for the 2.6 GeV, reversed field (left panel) and 4.2 GeV, normal field (right panel) running conditions. The

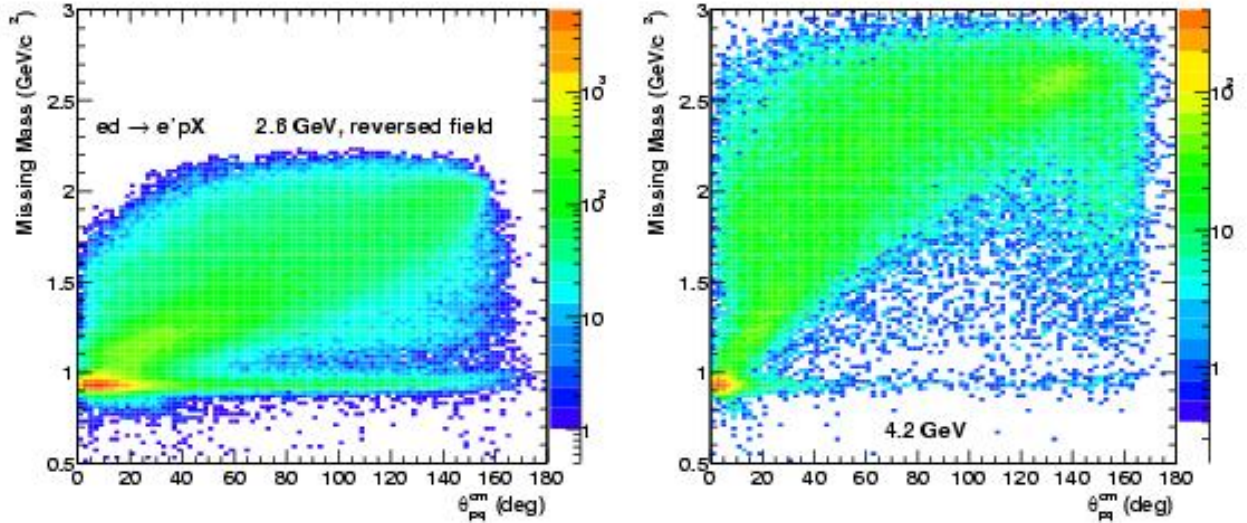


Figure 5: Missing mass versus θ_{pq}^{cm} for $ed \rightarrow e'pX$ for 2.6 GeV, reversed field (left panel) and 4.2 GeV (right panel).

ridge at the missing mass of the neutron (0.94 GeV) is clearly visible, well separated, and extends to large angle especially for the 2.6 GeV, reversed field data. We will be able to identify the missing neutron across the full kinematic range.

Momentum corrections have not yet been applied to the events analyzed here because we have found those corrections to have little effect on the results [25, 26]. In Reference [25] the neutron mass determined from the missing mass technique for the reaction $p(e, e'\pi^+)X$ was 0.93490 ± 0.00003 GeV/ c^2 before applying corrections and only increased to 0.93570 ± 0.00003 GeV/ c^2 after corrections. We will apply these corrections later. The method used is described in CLAS-NOTE 2001-18.

Vertex cuts were imposed on the electron and proton tracks so only events coming from the central part of the deuterium or proton target would be analyzed. Figure 6 shows the distribution of the z component of the electron vertex for a single data file from run 24029. The red lines are at the limits of the vertex cut for the deuteron target and the proton target.

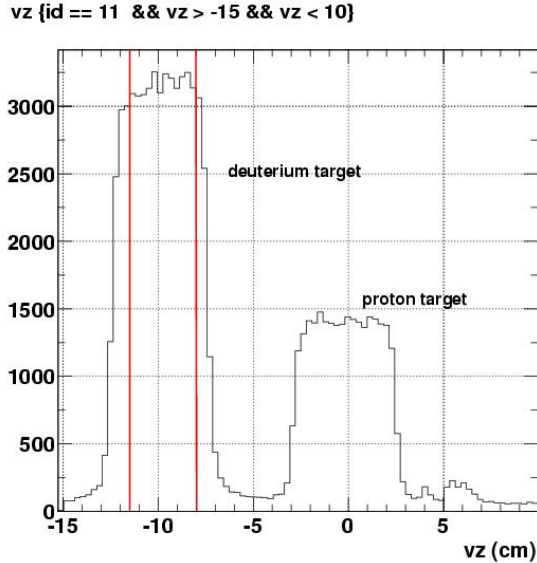


Figure 6: Distribution of the z component of the electron vertex. Red lines represent cuts imposed on all good events.

To account for any difference in the amount of beam striking the target for the two helicities we determined the beam charge asymmetry for each set of running conditions and then corrected our data for it. The beam charge asymmetry (BCA) is defined as the ratio of the normalized beam intensities for the two different beam helicities. We calculated the beam charge asymmetry using the inclusive (e, e') electron yields for positive (N_+) and negative (N_-) helicities with the following expression.

$$A_Q = \frac{N_+}{N_-} \quad (10)$$

The inclusive cross section has no helicity dependence and is more reliable than the Faraday cup readings [27]. Some of our results are shown below in Figure 7 for the 2.56-GeV, normal-torus-polarity running conditions. The average for these run conditions is $A_Q = 0.9952 \pm 0.0007$. The half-wave plate which determines the beam helicity was fixed during the E5 run period. This means we should see not shifts in the BCA, which is consistent with Figure 7.

The measurements of the $d(\vec{e}, e'p)n$ reaction in this proposed analysis are subject to radiative corrections. We are using a modified version of the program EXCLURAD written by Afanasev, *et al.* to perform those calculations [28]. This code applies a more sophisticated method than the usual approach of Mo and Tsai or Schwinger and takes into account the exclusive nature of our measurements [29, 30]. We have not yet applied those corrections to our data, but we have revised EXCLURAD so that it can be applied to these data. The code was originally written for the $p(e, e'\pi^+)X$ reaction and we have modified it for the $d(\vec{e}, e'p)n$ reaction. Some of this work is described in the Appendix.

4.3 Extracting Asymmetries

In this section we discuss several methods for extracting the asymmetries A'_{LT} , A_{LT} , and A_{TT} as defined in Equations 4-6. The first uses small angle bins to directly apply Equations 4-6 to the data and calculate all three asymmetries. The second method is based on calculating different moments of the data and takes

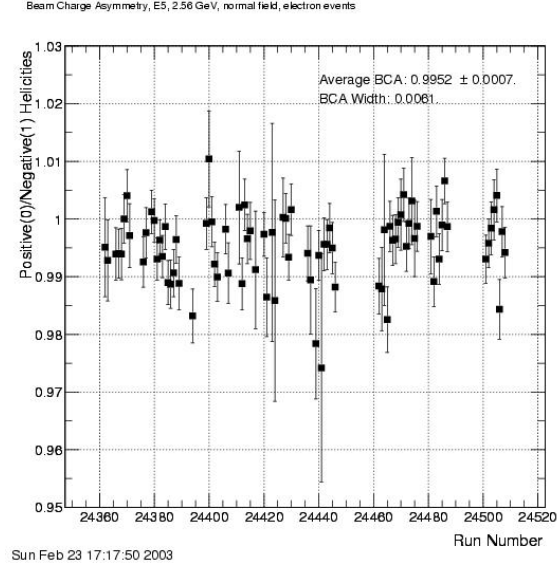


Figure 7: Beam charge asymmetry (BCA) for the 2.56-GeV, normal-torus-field-polarity running conditions.

advantage of the full angular coverage of CLAS to extract the three asymmetries. The third technique fits the out-of-plane angular distribution of the asymmetry and should yield the same results as the previous method for A'_{LT} , but does not apply to A_{LT} and A_{TT} .

The results from applying Equations 4-6 using small ($\pm 4^\circ$) angle bins around $\phi_{pq} = 90^\circ$ and $\phi_{pq} = 180^\circ$ are shown in the Figure 8 below. The results for A_{LT} show a large, negative asymmetry for $\theta_{pq}^{cm} < 30^\circ$ which decreases at larger angles where the uncertainties become significant. For A'_{LT} there is a small ($\approx 2\sigma$) excursion from zero in the range $\theta_{pq}^{cm} = 20^\circ - 30^\circ$ and the results are consistent with zero elsewhere. Note that the uncertainties are large on A'_{LT} which is expected to be small. The results for A_{TT} show a small, but significant asymmetry (about $4 - 5\sigma$) in the range $\theta_{pq}^{cm} = 0^\circ - 10^\circ$ which declines at larger angles.

We now develop the method to extract the asymmetries using the moments of the full ϕ_{pq} distribution measured with CLAS. The triply differential cross section for $d(\vec{e}, e'p)n$ can be written as

$$\frac{d^3\sigma}{d\nu d\Omega_e d\Omega_p} = \sigma^\pm = c[\rho_L f_L + \rho_T f_T + \rho_{LT} f_{LT} \cos(\phi_{pq}) + \rho_{TT} f_{TT} \cos(2\phi_{pq}) + h\rho'_{LT} f'_{LT} \sin(\phi_{pq})] \quad (11)$$

$$= \sigma_L + \sigma_T + \sigma_{LT} \cos \phi_{pq} + \sigma_{TT} \cos 2\phi_{pq} + h\sigma'_{LT} \sin \phi_{pq} \quad (12)$$

where the superscript on σ^\pm refers to the helicity, ϕ_{pq} is the angle between the plane defined by the incoming and outgoing electron momenta and plane defined by the ejected proton and neutron, the ρ 's depend only on the kinematics, f are the structure functions, c is proportional to the Mott cross section (see Equation 2), the σ 's are the partial cross sections for each component, and h is the helicity of the electron beam (± 1). To extract A'_{LT} consider the asymmetry

$$A(\phi_{pq}) = \frac{\sigma^+ - \sigma^-}{\sigma^+ + \sigma^-} \quad (13)$$

where the superscripts refer to the helicity of the electron beam. Substituting Equation 12 into Equation 13 one obtains

$$A(\phi_{pq}) = \frac{\sigma^+ - \sigma^-}{\sigma^+ + \sigma^-} = \frac{\sigma'_{LT} \sin \phi_{pq}}{\sigma_L + \sigma_T + \sigma_{LT} \cos \phi_{pq} + \sigma_{TT} \cos 2\phi_{pq}} \quad (14)$$

so for $\phi_{pq} = 90^\circ$ the asymmetry becomes

$$A(\phi_{pq} = 90^\circ) = A'_{LT} = \frac{\sigma_{90}^+ - \sigma_{90}^-}{\sigma_{90}^+ + \sigma_{90}^-} = \frac{\sigma'_{LT}}{\sigma_L + \sigma_T - \sigma_{TT}} \approx \frac{\sigma'_{LT}}{\sigma_L + \sigma_T} \quad (15)$$

The last approximation above will hold if σ_{TT} is small compared to σ_L or σ_T as has been observed [8, 12, 13].

Now consider taking the $\sin \phi_{pq}$ moment of the distribution for the two different choices of helicity.

$$\langle \sin \phi_{pq} \rangle_{\pm} = \frac{\int_0^{2\pi} \sigma^{\pm} \sin \phi_{pq} d\phi_{pq}}{\int_0^{2\pi} \sigma^{\pm} d\phi_{pq}} \quad (16)$$

$$= \frac{\int_0^{2\pi} (\sigma_L + \sigma_T + \sigma_{LT} \cos \phi_{pq} + \sigma_{TT} \cos 2\phi_{pq} + h\sigma'_{LT} \sin \phi_{pq}) \sin \phi_{pq} d\phi_{pq}}{\int_0^{2\pi} (\sigma_L + \sigma_T + \sigma_{LT} \cos \phi_{pq} + \sigma_{TT} \cos 2\phi_{pq} + h\sigma'_{LT} \sin \phi_{pq}) d\phi_{pq}} \quad (17)$$

By the orthogonality of sines and cosines all of the terms disappear except for the σ'_{LT} term in the numerator and the ϕ_{pq} -independent terms in the denominator. The result is

$$\langle \sin \phi_{pq} \rangle_{\pm} = \frac{\pm \sigma'_{LT}}{2(\sigma_L + \sigma_T)} \approx \pm \frac{A'_{LT}}{2} \quad (18)$$

where we have used Equation 6, $h = \pm 1$, and again neglected the contribution of σ_{TT} . To determine $\langle \sin \phi_{pq} \rangle_{\pm}$ for a given bin in Q^2 and θ_{pq}^{cm} or p_m from the data one uses

$$\langle \sin \phi_{pq} \rangle_{\pm} = \frac{1}{N_{\pm}} \sum_{i=1}^{N_{\pm}} \sin \phi_i \quad (19)$$

where the sum is over the ϕ_{pq} distribution of the data, i 's refer to individual events, and N_{\pm} refers to the number of events of each helicity.

In Equation 18, σ'_{LT} depends on θ_{pq}^{cm} , Q^2 , p_m or θ_{pq}^{cm} , but as a function of one of those variables, say θ_{pq}^{cm} , one expects to see behavior like that shown in Figure 9 below. The curve for one helicity is the opposite of the curve for the other helicity. However, acceptance effects can distort the expected distributions of

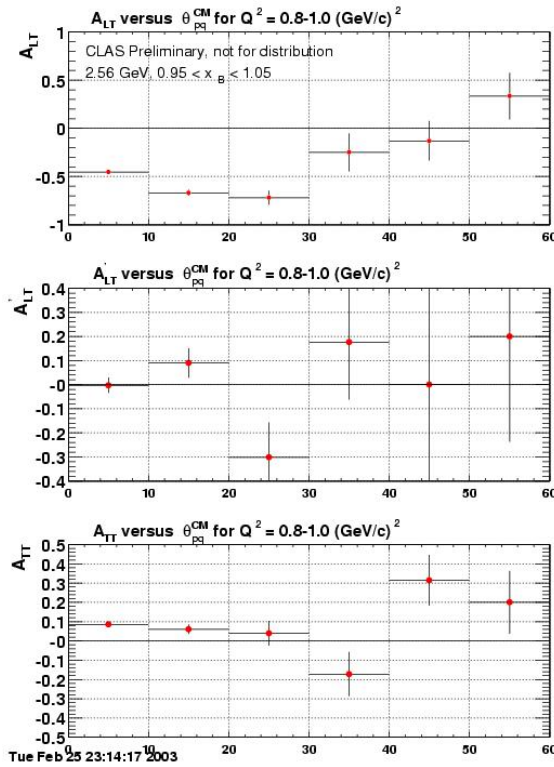


Figure 8: Asymmetries as a function of θ_{pq}^{cm} extracted using small angle bins.

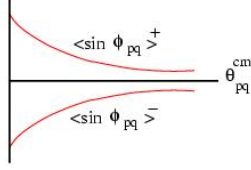


Figure 9: Schematic drawing showing the expected results for $\langle \sin \phi_{pq} \rangle_{\pm}$.

Equation 18 if the CLAS acceptance has a component that varies as $\sin \phi_{pq}$. In such a case this component will survive the integration in Equation 17 when it is multiplying the constant portion of the cross section (σ_L and σ_T terms in Equation 17). Such an acceptance effect is additive and shifts $\langle \sin \phi_{pq} \rangle_{\pm}$ up or down, so

$$\langle \sin \phi_{pq} \rangle_{\pm}^{meas} = \pm \frac{\sigma'_{LT}}{2(\sigma_L + \sigma_T)} + \alpha \quad (20)$$

where α is the additive acceptance correction. See the Appendix for more details. If one has measured this $\sin \phi_{pq}$ moment for each helicity then the results can be combined so

$$\langle \sin \phi_{pq} \rangle_{+}^{meas} - \langle \sin \phi_{pq} \rangle_{-}^{meas} = \frac{\sigma'_{LT}}{\sigma_L + \sigma_T} \approx A'_{LT} \quad (21)$$

and

$$\frac{\langle \sin \phi_{pq} \rangle_{+}^{meas} + \langle \sin \phi_{pq} \rangle_{-}^{meas}}{2} = \alpha \quad (22)$$

The asymmetry A'_{LT} is extracted with reduced sensitivity to acceptance corrections and the acceptance corrections have been measured from the data. This technique has been used by others for the $p(\bar{e}, e'\pi^+)n$ and $p(\bar{e}, e'p)\pi^0$ reactions [32, 33].

We have applied this analysis to our data and some preliminary results are shown in Figure 10. The two top panels show $\langle \sin \phi_{pq} \rangle_{+}^{meas}$ and $\langle \sin \phi_{pq} \rangle_{-}^{meas}$. The two distributions are not opposites of each other, implying there is a significant modification due to acceptance effects. The lower left panel shows the acceptance correction as a function of θ_{pq}^{cm} extracted by applying Equation 22. The acceptance correction α varies smoothly with θ_{pq}^{cm} and is in the range 4–12%. The lower right panel shows the asymmetry A'_{LT} determined by the difference between the two, helicity-dependent, $\sin \phi_{pq}$ distributions (see Equation 21). It reveals a significant, negative asymmetry at $\theta_{pq}^{cm} = 20 - 30^\circ$ that is 2–3 standard deviations away from zero. The asymmetry is consistent with zero in other θ_{pq}^{cm} bins within the measured uncertainty.

The two other asymmetries A_{LT} and A_{TT} can be extracted in a similar way. One can show that for A_{LT}

$$\langle \cos \phi_{pq} \rangle = \frac{\int_0^{2\pi} \sigma^{\pm} \cos \phi_{pq} d\phi}{\int_0^{2\pi} \sigma^{\pm} d\phi_{pq}} \quad (23)$$

$$= \frac{\int_0^{2\pi} (\sigma_L + \sigma_T + \sigma_{LT} \cos \phi_{pq} + \sigma_{TT} \cos 2\phi_{pq} + h\sigma'_{LT} \sin \phi_{pq}) \cos \phi_{pq} d\phi_{pq}}{\int_0^{2\pi} (\sigma_L + \sigma_T + \sigma_{LT} \cos \phi_{pq} + \sigma_{TT} \cos 2\phi_{pq} + h\sigma'_{LT} \sin \phi_{pq}) d\phi_{pq}} \quad (24)$$

$$= \frac{\sigma_{LT}}{2(\sigma_L + \sigma_T)} \quad (25)$$

Combining the definition of A_{LT} (recall Equation 4) with Equation 12 for the cross section and neglecting the small transverse-transverse (TT) piece one obtains

$$\langle \cos \phi_{pq} \rangle \approx \frac{A_{LT}}{2} \quad (26)$$

Notice there is no dependence on helicity here. For A_{TT} one follows a similar procedure to show

$$\langle \cos 2\phi_{pq} \rangle = \frac{\int_0^{2\pi} \sigma^{\pm} \cos 2\phi_{pq} d\phi}{\int_0^{2\pi} \sigma^{\pm} d\phi_{pq}} = \frac{\sigma_{TT}}{2(\sigma_L + \sigma_T)} \approx \frac{A_{TT}}{2} \quad (27)$$

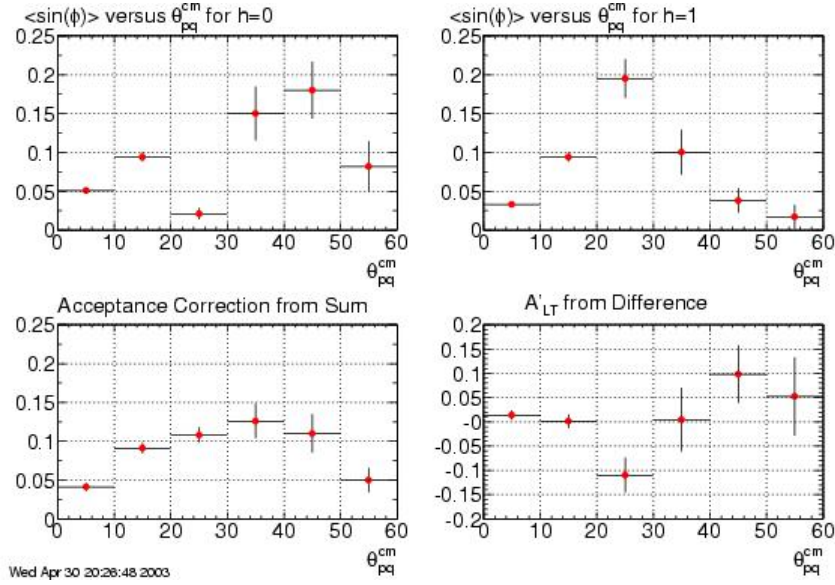


Figure 10: Preliminary results for $\langle \sin \phi_{pq} \rangle$ moments analysis for 2.56 GeV, normal field, not acceptance corrected, $0.8 < Q^2 < 1.0$ (GeV/c) 2 , $0.95 < x_B < 1.05$. The notation is $h = 0$ for positive helicity and $h = 1$ for negative helicity.

The figure below shows the asymmetries A_{LT} and A_{TT} extracted using the moments analysis and compared with the results using finite angle bins. The upper-left panel shows A_{LT} from the moments analysis and it reveals a large, negative asymmetry at $\theta_{pq}^{cm} = 0^\circ - 30^\circ$. This result is consistent with the finite-angle-bin measurement (lower-left panel), but has much better precision especially at large θ_{pq}^{cm} . The upper-right panel shows the results of the moment analysis for A_{TT} . There is a statistically significant positive asymmetry across the full angular range ($\theta_{pq}^{cm} = 0^\circ - 60^\circ$) for $\langle \cos 2\phi_{pq} \rangle$. There is good agreement with the finite-angle-bin analysis for the $0^\circ - 10^\circ$ bin and for $\theta_{pq}^{cm} = 30^\circ - 50^\circ$. In the intermediate angle bins the results differ, but the uncertainties on the finite-angle-bin results are large. It is worth noting here that we expect, based on previous results, that σ_{LT} and σ_{TT} will be small relative to σ_L and σ_T . The large asymmetries shown in Figure 11 include acceptance effects which have not yet been calculated so we can draw no conclusions yet about the true size of the acceptance-corrected asymmetries.

We investigated a third method for extracting A'_{LT} that takes advantage of the large acceptance of CLAS. Recall the expression for $A(\phi_{pq})$ (see Equation 14). The numerator in Equation 14 is proportional to $\sin(\phi_{pq})$ and the denominator is constant as long as σ_{LT} and σ_{TT} are small. If one forms the ratio of different helicities

$$A(\phi_{pq}) = \frac{\sigma^+ - \sigma^-}{\sigma^+ + \sigma^-} = \frac{N^+ - N^-}{N^+ + N^-} \frac{1}{A_Q} = \frac{\sigma'_{LT} \sin \phi_{pq}}{\sigma_L + \sigma_T + \sigma_{LT} \cos \phi_{pq} + \sigma_{TT} \cos 2\phi_{pq}} \quad (28)$$

where A_Q is the beam charge asymmetry, then the distribution should have a sinusoidal dependence on ϕ if σ_{LT} and σ_{TT} are small relative to σ_T and σ_L . We have calculated this ratio and some preliminary results are shown in Figure 12 for four different angle bins in the range $Q^2 = 0.8 - 1.0$ (GeV/c) 2 . The distributions were fitted with a sine curve and the results are shown on the figure. The fits all have acceptable reduced χ^2 . We also tried fitting a more complex function that included the $\cos \phi_{pq}$ and $\cos 2\phi_{pq}$ terms in the denominator of Equation 28. We found the contributions from σ_{LT} and σ_{TT} were consistent with zero and there was no significant improvement to the fit.

We compared the three different methods for measuring A'_{LT} and show the results in Figure 13. The top panel shows the angular distribution in θ_{pq}^{cm} measured using the $\sin \phi_{pq}$ moments of the distribution, the middle panel is from the fits to $A(\phi_{pq})$, and the bottom panel is from differences between small angle bins. It is worth noting again the first two methods take advantage of the large acceptance of CLAS while the last method ignores much of the data. The results in Figure 13 are for the range $Q^2 = 0.8 - 1.0$ (GeV/c) 2 .

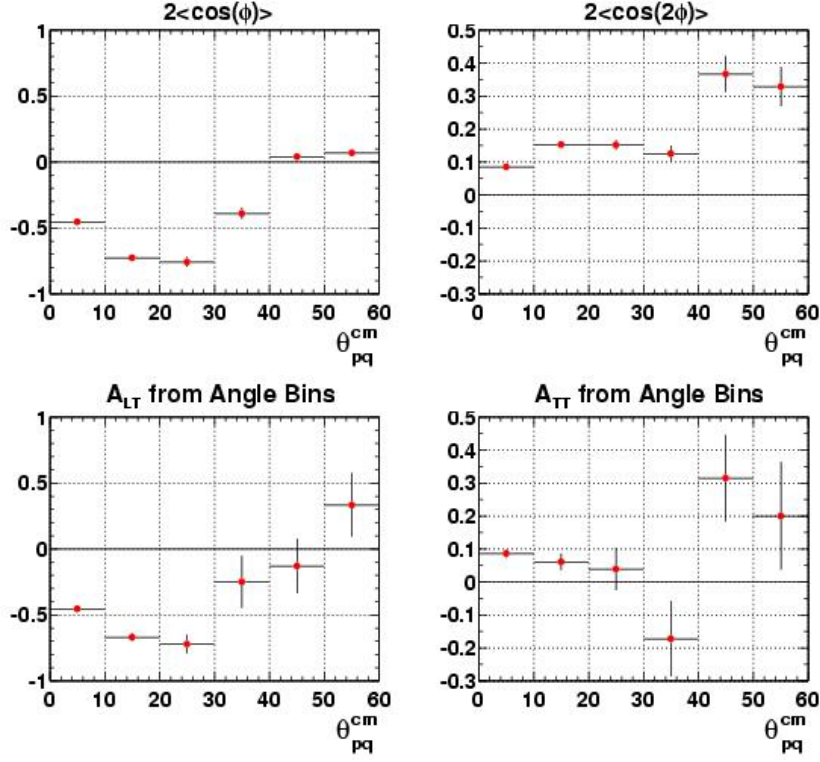


Figure 11: Comparison of A_{LT} and A_{TT} determined from an analysis of the ϕ moments of the distribution (upper panel) compared with the results from using small angle bins.

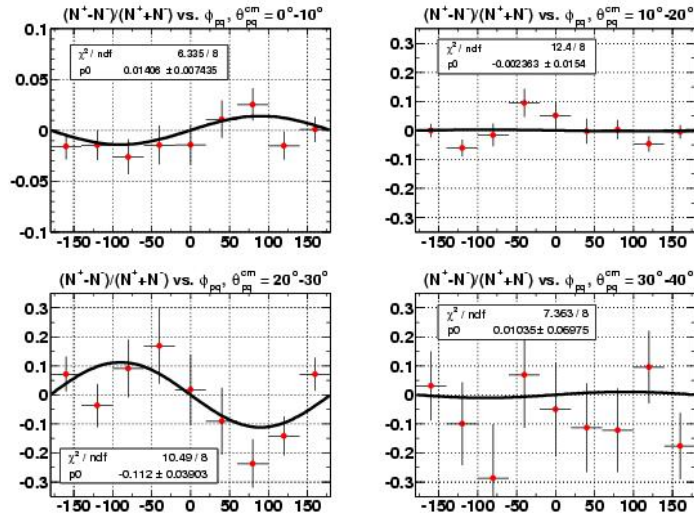


Figure 12: Preliminary results for ϕ dependence of A'_{LT} using the helicity ratio technique.

The top two panels are very consistent with each other. The values of A'_{LT} in each angle bin agree for both methods as well as the size of the uncertainties in each angle bin. It is worth noting how A'_{LT} goes from small and positive for $\theta_{pq}^{cm} = 0^\circ - 10^\circ$ to large and negative for $\theta_{pq}^{cm} = 20^\circ - 30^\circ$. This is clearly seen in the shapes of the ϕ_{pq} distributions in Figure 12 in the upper-left and lower-left panels. We expect the $\sin \phi_{pq}$

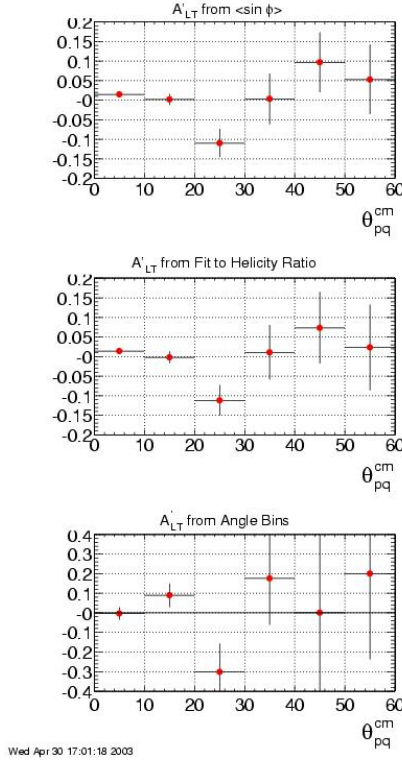


Figure 13: Comparison of A'_{LT} extracted using different analysis techniques. The calculation is not corrected for the CLAS acceptance.

moments and the $A(\phi_{pq})$ methods to be consistent; they represent the same quantity extracted from the same data set. The results in the bottom panel are consistent with the others within the uncertainties. We do not expect the results in the bottom panel to match as well since we are using a subset of the data which also means the uncertainties will be larger. We conclude that these methods are self-consistent and the $\sin \phi_{pq}$ moments analysis and the fit to $A(\phi_{pq})$ are equivalent methods. It is worth noting that the angular distribution shown here for $Q^2 = 0.8 - 1.0$ (GeV/c) 2 is a small fraction of the E5 data that covers the range $Q^2 = 0.2 - 5.0$ (GeV/c) 2 .

There are other methods for checking our analysis. During the E5 run period the data were collected simultaneously from the proton target and will be compared with other CLAS analyses [32, 34]. The kinematic regions probed by the different E5 run conditions overlap each other so our results can be compared with different beam energies and/or torus magnet settings. As a final test of the quality of the analysis we make a preliminary comparison of our results with theory. In Figure 14 below we show A'_{LT} as function of θ_{pq}^{cm} calculated from the $\sin \phi_{pq}$ moments analysis along with a calculation from H. Arenhövel that includes relativistic effects, meson-exchange currents, isobar configurations, and final-state interactions [35]. The magnitude and sign of the asymmetry are reproduced by the calculation. However, the shape of the data is different; it is narrower and shifted to smaller angles. Note, this comparison is at $Q^2 = 0.8 - 1.0$ (GeV/c) 2 which is near the limit of validity of the Arenhövel calculation. These differences hint at the need for improvements to the hadronic model of nuclear physics.

We have begun to address the sources of uncertainty in our investigation. The CLAS has a finite angular resolution which becomes more important for small θ_{pq}^{cm} , *i.e.* when the emitted proton is moving nearly parallel to the 3-momentum transfer. In the limit of $\theta_{pq}^{cm} = 0$, the azimuthal angle, ϕ_{pq} is undefined. At small θ_{pq}^{cm} our determination of ϕ_{pq} will become unreliable because of this angular resolution. We have examined this ‘pointing’ error using the elastic scattering off the proton with the hydrogen target. We extracted the difference between the measured proton momentum and the 3-momentum transfer determined

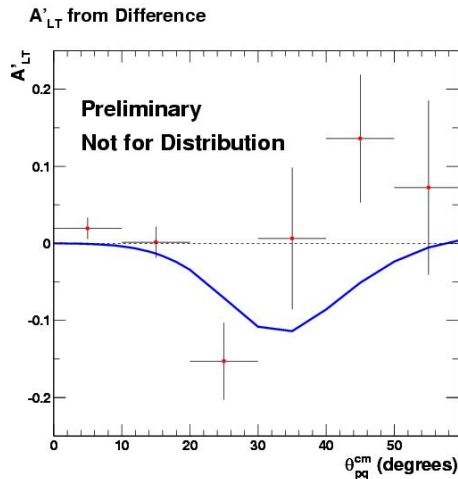


Figure 14: Comparison of results for A'_{LT} at 2.56 GeV, normal field, $0.8 < Q^2 < 1.0$ (GeV/c) 2 , $0.95 < x_B < 1.05$ (not acceptance corrected). The measured asymmetry is corrected for the beam polarization. The blue curve is a calculation by Arenhövel.

by incoming and outgoing electron momenta. The width of the distribution is about $\sigma \approx 0.6^\circ$ and is symmetric about the origin. We will address this question along with other sources of uncertainty including the acceptance calculations as the project progresses.

Much work remains. We are not yet applying the corrections to remove the distortions of the data caused by CLAS such as momentum corrections, energy loss, corrections, *etc.* We are also improving data selection. Fiducial cuts on the electron and proton to define the active volume of the CLAS are being developed. Calculation of the acceptance of CLAS is just beginning. This step is critical for understanding the f_{LT} and f_{TT} results. It is less important for the f'_{LT} analysis because using the ratio of different helicities to calculate A'_{LT} reduces many of the systematic uncertainties. We have only begun investigating the sources of uncertainty in our analysis. The ‘pointing’ error described above and radiative corrections are two examples.

5 Conclusions

We propose to extract the structure functions f_{LT} , f_{TT} , and f'_{LT} of the deuteron in the region $Q^2 = 0.2 - 5.0$ (GeV/c) 2 using out-of-plane measurements recorded during the E5 running period. These data will challenge the existing ‘standard model’ of nuclear physics in a transition region in Q^2 where many expect the model to begin to break down and quark and gluon degrees of freedom to manifest themselves. More specifically, these data will test our understanding of relativistic corrections, meson-exchange currents, isobar configurations, and final-state interactions.

Our preliminary analysis of the data from the E5 running period shows that we can extract the structure functions with good to excellent precision. We have found this can be done using the different azimuthal moments of the data: $\langle \cos \phi_{pq} \rangle$ for f_{LT} , $\langle \cos 2\phi_{pq} \rangle$ for f_{TT} , and $\langle \sin \phi_{pq} \rangle$ for f'_{LT} . The fifth structure function f'_{LT} can be extracted from the moment analysis and also from fitting the A_ϕ asymmetry. Both methods give equivalent results. This last structure function is small and likely the most difficult to measure so it provides a stringent test of our techniques. Our preliminary results show that asymmetries as large as 0.15 can be expected for f'_{LT} . The statistical uncertainties range in size from 0.01 at small θ_{pq}^{cm} to 0.04 at $\theta_{pq}^{cm} \approx 30^\circ$. The results shown here for f'_{LT} represent only a small fraction of the total data set.

References

- [1] PAC 14 Few-Body Workshop, Williamsburg, VA, July, 1998.
- [2] S.Jeschonnek, Phys. Rev **C63** 034609 (2001).
- [3] S.Jeschonnek and T.W.Donnely, Phys. Rev. **C57** 2438 (1998).
- [4] S.Jeschonnek and J.W.Van Orden, Phys. Rev. **C62** 044613 (2000).
- [5] F.Ritz, H.Goller, Th. Wilbois, and H.Arenhövel, Phys. Rev. **C55**, 2214 (1997).
- [6] R.Gilman and F.Gross, J.Phys.G: Nucl. Part. Phys. **28**, R37 (2002).
- [7] ‘Opportunities in Nuclear Science: A Long-Range Plan for the Next Decade’, DOE/NSF Nuclear Science Advisory Committee, April 2002, p. 30.
- [8] S.Gilad, W.Bertozzi, and Z.-L.Zhou, Nucl. Phys. **A631** 276c (1998).
- [9] S. Boffi, C. Giusti, F. D. Pacati, and M. Radici, *Electromagnetic Response of Atomic Nuclei*, Oxford University Press, Oxford, England, 1996.
- [10] S.M.Dolfini *et al.*, Phys. Rev. **C60** 064622 (1999).
- [11] S.M.Dolfini, *et al.*, Phys. Rev. **C51** 3479 (1995).
- [12] T.Tamae, *et al.*, Phys. Rev. Lett. **59** 2919 (1987).
- [13] M. van der Schaar *et al.*, Phys. Rev. Lett. **68**, 776 (1992).
- [14] H.J.Bulten, *et al.*, Phys. Rev. Lett. **74** 4775 (1995).
- [15] E.Hummel and J.A.Tjon, Phys. Rev. Lett. **63**, 1788 (1989); Phys. Rev. **C42** 423, (1990).
- [16] H.Arenhövel, Nucl. Phys. **A365**, 349 (1981).
- [17] W.Fabian and H.Arenhövel, Nucl. Phys. **A314**, 252 (1979).
- [18] D.Jordan *et al.*, Phys. Rev. Lett. **76** 1579 (1996).
- [19] J.E.Ducret, *et al.*, Phys. Rev. **C49** 1783 (1994).
- [20] F.Frommberger, *et al.* Phys. Lett. **B339** 17 (1994).
- [21] P.E.Ulmer, *et al.*, Phys. Rev. Lett. **89**, 062301, 2002.
- [22] H.Arenhövel, W.Leidemann and E.L.Tomusiak, Phys. Rev. **C52**, 1232 (1995).
- [23] Z.-L. Zhou *et al.*, Phys. Rev. Lett. **87** 172301 (2001).
- [24] C.Hadjidakis, private communication.
- [25] J.Lachniet, ‘Report on momentum corrections in E5’, <http://clasweb.jlab.org/cgi-bin/ENOTE/enote.pl?nb=e5&action=view&page=109>, [Accessed 10 July, 2003].
- [26] J.Lachniet, ‘A second look at momentum corrections’, <http://clasweb.jlab.org/cgi-bin/ENOTE/enote.pl?nb=e5&action=view&page=166>, [Accessed 10 July, 2003].
- [27] M.Anghinolfi, CLAS-Note 2001-020.
- [28] A.Afanasev, I.Akushevich, V.Burkert, and K.Joo, Phys.Rev., **D66**, 074004, 2002.
- [29] L.W.Mo and Y.S.Tsai, Rev. Mod. Phys., **41**, 205, 1969.
- [30] J.Schwinger, Phys. Rev., **76**, 898, 1949.

- [31] Juan Cornejo, *radiative corrections, external and internal bremsstrahlung factors*, Retrieved on January 30, 2003 from http://www.calstatela.edu/academic/nuclear_physics/schwin12_extbrems.html.
- [32] K.Joo and C.Smith, CLAS Analysis Note 2001-009.
- [33] H.Avakian, CLAS Analysis Note 2002-101.
- [34] K.Joo and C.Smith, private communication.
- [35] H.Arenhövel, private communication.

A Appendix

A.1 Radiative Corrections

To test our modifications to EXCLURAD we will compare them with the more traditional approaches. Below we describe how to relate the parameters of the Schwinger-style calculation with the approach used in EXCLURAD. In the Schwinger method one calculates the radiative correction for the scattering of an electron in a Coulomb field. This corresponds to inclusive electron scattering. An essential step in the calculation is to integrate over the radiative tail of the energy of a scattered electron to arrive at a correction factor for the yield lost to the emission of photons. The parameters of that integration are defined in Figure 15 [31]. The parameter ΔE is the energy range over which the integral is performed (starting at the

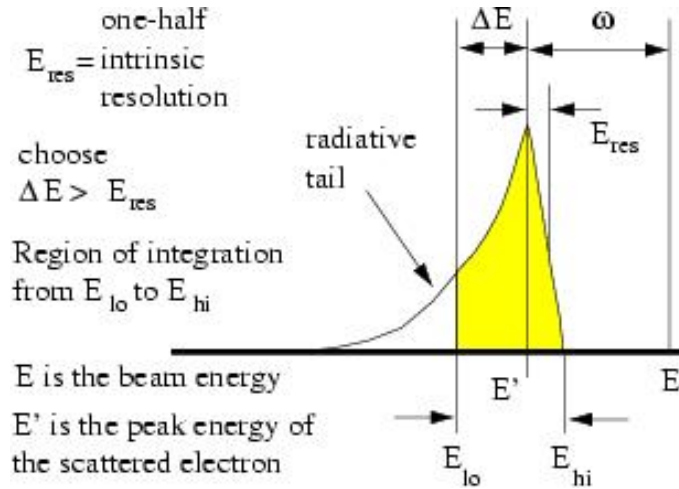


Figure 15: Energy spectrum of scattered electron showing definitions of quantities used in Schwinger radiative correction calculation.

unradiated energy of the electron) to estimate the yield lost to radiated photons.

Afanasev, *at al.* follow an analogous procedure in their more sophisticated approach [28]. They integrate over the radiative tail of the scattered electron, but they perform the integration in terms of the covariant ‘inelasticity’ v defined as

$$v = \Lambda^2 - m_u^2 \quad (29)$$

where m_u is the mass of the undetected hadron and Λ is the four-momentum of the missing or undetected particles. The quantity v describes the missing mass due to the emission of a bremsstrahlung photon and can be rewritten as

$$v = W^2 + m_h^2 - m_u^2 - 2WE_h \quad (30)$$

where W is the mass of the system recoiling against the electron, m_h is the mass of the detected hadron, and E_h is the center-of-mass energy of the detected hadron. To determine the relationship between ΔE and

v consider the usual expression for W^2

$$W^2 = M^2 + 2M(E - E') - Q^2 \quad (31)$$

where

$$Q^2 \approx 4EE' \sin^2 \frac{\theta}{2} \quad (32)$$

M is the target mass, and θ is the electron scattering angle. However, for an event with a radiated photon, the measured energy of the scattered electron is not E' , but some lower energy

$$E_{lo} = E' - \Delta E \quad (33)$$

so W for this event will not be ‘correct’. The new value of W is

$$W_{rad}^2 = M^2 + 2M(E - E_{lo}) - 4EE_{lo} \sin^2 \frac{\theta}{2} \quad (34)$$

Using Equations 33 and 34 in the expression for v in Equation 30 one obtains the following function of ΔE .

$$v = M^2 + 2M(E - E' + \Delta E) - 4E(E' + \Delta E) \sin^2 \frac{\theta}{2} + m_h^2 - m_u^2 - 2E_h \sqrt{M^2 + 2M(E - E' + \Delta E) - 4E(E' + \Delta E) \sin^2 \frac{\theta}{2}} \quad (35)$$

This expression can be re-arranged so

$$v = W_0^2 + m_h^2 - m_u^2 + 2\Delta E(M + 2E \sin^2 \frac{\theta}{2}) - 2E_h \sqrt{W_0^2 + 2\Delta E(M + 2E \sin^2 \frac{\theta}{2})} \quad (36)$$

where

$$W_0^2 = M^2 + 2M(E - E') - 4EE' \sin^2 \frac{\theta}{2} \quad (37)$$

and the quantities E , E' , and θ are determined by the electron kinematics. The hadron energy E_h is determined by the choice of the angle of the outgoing hadron relative to \vec{q} , the three-vector of the momentum transfer. The masses M , m_h , and m_u are all known.

As an example of applying Equation 35 consider the following kinematics. The results of the calculation

$E = 2.558$ GeV	$E' = 2.345$ GeV	$\theta = 14.84^\circ$
$m_h = 0.938$ GeV	$m_u = 0.940$ GeV	$\theta_h^{cm} = 45^\circ$
$M = 1.876$ GeV	$Q^2 = 0.52$ (GeV/c) ²	$W = 1.93$ GeV

Table 1: Kinematics for calculating $v(\Delta E)$.

are shown in Figure 6. The dependence of v on ΔE is almost linear implying the importance of that term in Equation 36 over the sum of all the other terms.

A.2 Acceptance Effects in $\langle \sin \phi_{pq} \rangle_{\pm}$

To more clearly understand Equation 20 which relates $\langle \sin \phi_{pq} \rangle_{\pm}$ to A'_{LT} and the acceptance recall again the expression for the differential cross section for $d(\vec{e}, e'p)n$.

$$\frac{d^3\sigma}{dvd\Omega_e d\Omega_p} = \sigma^{\pm} = c[\rho_L f_L + \rho_T f_T + \rho_{LT} f_{LT} \cos(\phi_{pq}) + \rho_{TT} f_{TT} \cos(2\phi_{pq}) + h\rho'_{LT} f'_{LT} \sin(\phi_{pq})] \quad (38)$$

$$= \sigma_L + \sigma_T + \sigma_{LT} \cos \phi_{pq} + \sigma_{TT} \cos 2\phi_{pq} + h\sigma'_{LT} \sin \phi_{pq} \quad (39)$$

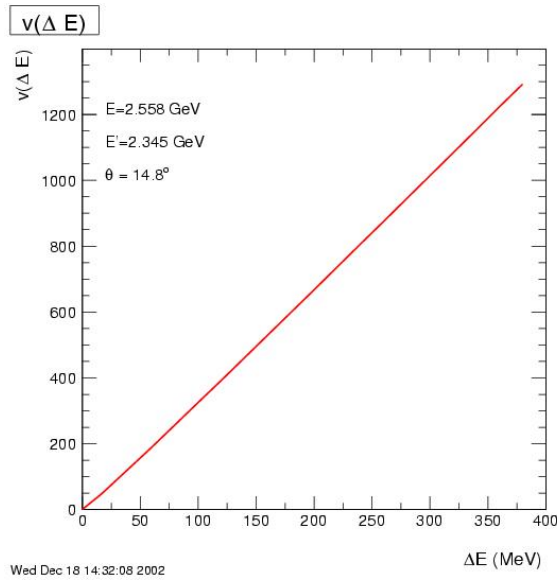


Figure 16: Dependence of v on ΔE for the kinematics listed in Table 1.

The $\sin \phi_{pq}$ moment of the data at a given Q^2 and θ_{pq}^{cm} or p_m is defined by the following expression.

$$\langle \sin \phi_{pq} \rangle_{\pm} = \frac{\int_0^{2\pi} \sigma^{\pm} \sin \phi_{pq} d\phi}{\int_0^{2\pi} \sigma^{\pm} d\phi} \quad (40)$$

Now let

$$\sigma^{\pm} = \kappa \epsilon(\phi_{pq}) N^{\pm}(\phi_{pq}) \quad (41)$$

where N^{\pm} is the number of counts for each helicity, ϵ is the CLAS acceptance and may vary with ϕ_{pq} , and κ contains all the other helicity-independent, kinematic factors needed to determine cross sections. In turn, N^{\pm} is composed of different longitudinal and transverse components so

$$N^{\pm}(\phi_{pq}) = N_L^{\pm} + N_T^{\pm} + N_{LT}^{\pm} \cos \phi_{pq} + N_{TT}^{\pm} \cos 2\phi_{pq} + h N_{LT}^{\pm} \sin \phi_{pq} \quad (42)$$

Hereafter, we will suppress the \pm superscript for clarity and it will be assumed that all N 's depend on the helicity. Finally, the CLAS acceptance as a function of ϕ_{pq} at a given Q^2 and θ_{pq}^{cm} or p_m can be expressed as

$$\epsilon(\phi_{pq}) = A_0 + \sum_{m=1}^{\infty} (a_m \sin m\phi_{pq} + b_m \cos m\phi_{pq}) \quad (43)$$

where we have taken advantage of the completeness of the sines and cosines. We expect any ϕ_{pq} dependence in the CLAS acceptance to vary slowly so we approximate it by taking the sum in Equation 43 up to $m = 2$ so

$$\epsilon(\phi_{pq}) = A_0 + a_1 \sin \phi_{pq} + b_1 \cos \phi_{pq} + a_2 \sin 2\phi_{pq} + b_2 \cos 2\phi_{pq} \quad (44)$$

Substituting Equations 41, 42, and 44 into Equation 40 one obtains (after doing some algebra and some integrals) the following expression

$$\langle \sin \phi_{pq} \rangle_{\pm} = \frac{(N_L + N_T - \frac{N_{TT}}{2})a_1 + \frac{N_{LT}a_2}{2} \pm N'_{LT}A_0}{2(N_L + N_T)A_0 + N_{LT}b_1 + N_{TT}b_2 + N'_{LT}a_1} \quad (45)$$

where we have used $h = \pm 1$. In the numerator, N_{TT} and N_{LT} are both much less than $N_L + N_T$ so we can neglect their contribution. We retain the N'_{LT} term since since it will survive when we take the difference

between the moments for the positive and negative helicities (the N_{TT} and N_{LT} terms will cancel in the difference). In the denominator, we can apply the same reasoning and neglect the N_{LT} and N_{TT} terms. Here we can also neglect the N'_{LT} term because it will have a small effect on the final difference. The result is

$$\langle \sin \phi_{pq} \rangle^\pm = \frac{(N_L + N_T)a_1 + N'_{LT}A_0}{2(N_L + N_T)A_0} \quad (46)$$

$$= \frac{a_1}{2A_0} + \frac{N'}{2(N_L + N_T)} \quad (47)$$

$$= \alpha + \frac{\sigma'_{LT}}{2(\sigma_L + \sigma_T)} \quad (48)$$

which is the form of Equation 20. We have used Equation 41 to eliminate the N 's and labeled the first term α to be consistent with the text.